

Using the Zeldovich dynamics to test expansion schemes

P. Valageas

Service de Physique Théorique, CEA Saclay, 91191 Gif-sur-Yvette, France

Received / Accepted

Abstract. We apply to the simple case of the Zeldovich dynamics various expansion schemes which may be used to study gravitational clustering. Using the well-known exact solution of the Zeldovich dynamics we can compare in details the predictions of these various perturbative methods with the exact non-linear result. Besides, we can study their convergence properties and their behavior at high orders. We find that most systematic expansions fail to recover the decay of the response function into the highly non-linear regime. “Linear methods” lead to increasingly fast growth in the highly non-linear regime for higher orders, except for Padé approximants which give a bounded response at any order. “Non-linear methods” manage to obtain some damping at one-loop order but they fail at higher orders. We note that, although it recovers the exact Gaussian damping, a resummation performed in the high- k limit is not well justified as the generation of non-linear power does not originate from a finite range of wavenumbers (hence there is no simple separation of scales). No method is able to recover the relaxation of the matter power-spectrum at highly non-linear scales. It is possible to impose in a somewhat ad-hoc fashion a Gaussian cutoff, which agrees with the exact two-point functions for two different times. However, this cutoff is not directly related to the clustering of matter and disappears in exact equal-time statistics such as the commonly used matter power-spectrum. On a quantitative level, we find that on weakly non-linear scales the usual perturbation theory and non-linear schemes to which one adds an ansatz for the response function with such a Gaussian cutoff are the two most efficient methods. We can expect these results to hold for the gravitational dynamics as well (this has been explicitly checked at one-loop order) since the structure of the equations of motion is identical for both dynamics.

Key words. gravitation; cosmology: theory – large-scale structure of Universe

1. Introduction

The growth of large-scale structures in the Universe through the amplification of small primordial fluctuations by gravitational instability is a key ingredient of modern cosmology (Peebles 1980). This process can be used to constrain cosmological parameters through the dependence of the matter power-spectrum on scale and redshift. For instance, observations of highly non-linear objects such as clusters of galaxies can help constrain the normalization of the matter power-spectrum and the average matter density (Oukbir & Blanchard 1992; Younger et al. 2005). Indeed, although theoretical predictions are not very accurate on these small scales, one can still derive useful constraints because they are very rare objects so that their dependence on cosmological parameters is very steep. Alternative probes such as baryonic acoustic oscillations (Eisenstein et al. 1998, 2005) or weak lensing surveys (Munshi et al. 2007; Massey et al. 2007) focus on weakly non-linear scales where they aim to measure the matter distribution through its power-spectrum or two-point correlation, which are sensitive to typical fluctuations. In such cases, one needs an accurate theoretical prediction to de-

rive useful constraints on cosmology. This problem is usually tackled through N-body simulations or perturbative expansions for scales not too far from the linear regime (Bernardeau et al. 2002). However, numerical simulations are rather costly and analytical methods may have the advantage to provide a better understanding of the physics at work. Besides, at such rather large scales a hydrodynamical description should be sufficient (i.e. one neglects shell-crossing) which facilitates analytical approaches as one can use the continuity and Euler equations instead of the Vlasov equation. Therefore, there has been recently a renewed interest in perturbation theory to devise analytical methods which could exhibit a good accuracy on weakly non-linear scales in order to be used for such observational probes (Crocce & Scoccimarro 2006a,b; Valageas 2007; McDonald 2007; Matarrese & Pietroni 2007).

Thus, Crocce & Scoccimarro (2006a,b) found that one can perform a partial resummation of the diagrammatic series which appears in the standard perturbative expansion to obtain a response function which decays into the non-linear regime as expected (whereas the standard expansion grows as a polynomial of increasing order as we truncate the series at higher order). Moreover, this result

agrees well with numerical simulations and can be used as an intermediate tool to obtain a more accurate prediction for the matter power-spectrum than with the usual perturbation theory (Crocce & Scoccimarro 2007). On the other hand, Valageas (2007) presented a path-integral formalism so that the system is fully defined by its action S (or its partition function Z). Then, one can apply usual tools of field theory such as large- N expansions (similar to a semi-classical expansion over powers of \hbar or a generalization to N fields) to derive the matter power-spectrum (Valageas 2007). Note that this method also applies to highly non-linear scales described by the Vlasov equation (Valageas 2004). Next, Matarrese & Pietroni (2007) recently proposed an alternative method based on the path-integral formalism where one considers the dependence of the system on a large-wavenumber cutoff Λ . This gives rise to a new set of equations and by taking the limit $\Lambda \rightarrow \infty$ one recovers the original system. These various methods may be seen as different reorganizations of the standard perturbative expansion. Of course, they all involve some truncation at some stage (otherwise the problem would be exactly solved) and they are all consistent up to that order (i.e. they only differ by higher-order terms).

In order to check the range of validity of such expansions one must compare their predictions with N-body simulations (and assume for observational purposes that the accuracy remains the same for close cosmological parameters). This is not very convenient since simulations themselves may be of limited accuracy. Besides, the behaviors of other two-point functions than the power-spectrum $P(k)$, such as the response function and self-energies and especially different-time functions such as $\langle \delta(\mathbf{x}_1, t_1) \delta(\mathbf{x}_2, t_2) \rangle$ with $t_1 \neq t_2$, have not been analyzed in details from N-body simulations (which do not give a direct access either to self-energies). Therefore, it is interesting to investigate these theoretical methods applied to a simpler dynamics which can be solved exactly. Then, one can compare in details the predictions of various expansion schemes with the exact non-linear results. Moreover, from the exact two-point functions one can reconstruct such expansion schemes in a direct manner without computing high-order diagrams which involve many integrals, simply by expanding back the exact non-linear result. In this way one can more easily investigate the convergence properties of these expansions and the behavior of high-order terms. A simple dynamics which can be solved exactly but which remains close to the gravitational dynamics (at least up to weakly non-linear scales) is provided by the Zeldovich approximation (Zeldovich 1970; Gurbatov et al. 1989; Shandarin & Zeldovich 1989). The latter was originally devised as an approximation to the gravitational dynamics. Here we take a different point of view as we modify the equations of motion so that the system is exactly given by the simple Zeldovich dynamics. Then, we apply to these new equations of motion various methods which can be applied to both dynamics (and to other stochastic dynamics such as the Navier-Stokes equations). Taking advantage of the exact results which can be obtained for the Zeldovich

dynamics and its simpler properties we study in details the accuracy and the general properties of these expansion schemes. This should shed light on the behavior of these methods applied to the gravitational dynamics because both dynamics exhibit similar equations of motion and these expansions apply in identical manner to both systems.

This article is organized as follows. First, in sect. 2 we derive the equations of motion associated with the Zeldovich dynamics and their linear solution. Next, in sect. 3 we obtain the path-integral formulation of this system, starting from either the differential form or the integral form of the equations of motion, in order to make the connection with different approaches used in the literature. Then, we briefly describe how some expansion schemes can be built from this path-integral formalism, such as large- N expansions in sect. 4 and evolution equations with respect to a high- k cutoff in sect. 5. Before investigating such methods we first derive in sect. 6 the exact non-linear two-point functions which can be obtained from the well-known exact solution of the Zeldovich dynamics. Then, we describe the behavior of standard perturbation theory in sect. 7 and of the steepest-descent method (built from a large- N expansion) in sect. 8. Next, we discuss in sect. 9 the high- k resummation proposed by Crocce & Scoccimarro (2006b) to improve the behavior of such expansion schemes. We turn to the 2PI effective action method in sect. 10 (a second approach built from a large- N expansion) and to simple non-linear schemes associated with this expansion in sect. 11. We investigate simple non-linear schemes associated with the dependence on a high- k cutoff in sect. 12. Finally, we study in sect. 13 the quantitative predictions on weakly non-linear scales of these methods at one-loop order and we conclude in sect. 14.

2. Equations of motion

2.1. Zeldovich approximation

At scales much larger than the Jeans length both the cold dark matter and the baryons can be described as a pressureless dust. Then, we can neglect orbit crossings and use a hydrodynamical description governed by the equations of motion (Peebles 1980):

$$\frac{\partial \delta}{\partial \tau} + \nabla \cdot [(1 + \delta)\mathbf{v}] = 0, \quad (1)$$

$$\frac{\partial \mathbf{v}}{\partial \tau} + \mathcal{H}\mathbf{v} + (\mathbf{v} \cdot \nabla)\mathbf{v} = -\nabla\phi, \quad (2)$$

$$\Delta\phi = \frac{3}{2}\Omega_m \mathcal{H}^2 \delta, \quad (3)$$

where $\tau = \int dt/a$ is the conformal time (and a the scale factor), $\mathcal{H} = d \ln a / d\tau$ the conformal expansion rate and Ω_m the matter density cosmological parameter. Here δ is the matter density contrast and \mathbf{v} the peculiar velocity. Since the vorticity field decays within linear theory (Peebles 1980) we take the velocity to be a potential field

so that \mathbf{v} is fully specified by its divergence θ or by its potential χ with:

$$\theta = \nabla \cdot \mathbf{v}, \quad \mathbf{v} = -\nabla \chi \quad \text{whence} \quad \theta = -\Delta \chi. \quad (4)$$

In the linear regime one finds that the linear growing mode satisfies:

$$\theta_L = -f\mathcal{H}\delta_L \quad \text{whence} \quad \phi_L = \frac{3\Omega_m\mathcal{H}}{2f}\chi_L, \quad (5)$$

where $f(\tau)$ is defined from the linear growing rate $D_+(\tau)$ of the density contrast by:

$$f = \frac{d \ln D_+}{d \ln a} = \frac{1}{\mathcal{H}} \frac{d \ln D_+}{d\tau}, \quad (6)$$

and $D_+(\tau)$ is the growing solution of:

$$\frac{d^2 D_+}{d\tau^2} + \mathcal{H} \frac{dD_+}{d\tau} = \frac{3}{2} \Omega_m \mathcal{H}^2 D_+. \quad (7)$$

If we make the approximation that the relation (5) remains valid in the non-linear regime, that is we replace the Poisson equation (3) by the second eq.(5): $\phi = 3\Omega_m\mathcal{H}\chi/2f$, then we obtain for the Euler equation (2):

$$\frac{\partial \mathbf{v}}{\partial \tau} + \left(1 - \frac{3}{2} \frac{\Omega_m}{f}\right) \mathcal{H} \mathbf{v} + (\mathbf{v} \cdot \nabla) \mathbf{v} = 0. \quad (8)$$

Obviously, as shown by eq.(8), within this approximation the velocity field now evolves independently of the density field. As is well known (Gurbatov et al. 1989), the approximation (8) is actually identical to the Zeldovich approximation. Indeed, a change of variables for the velocity field yields:

$$\frac{\partial \mathbf{u}}{\partial D_+} + (\mathbf{u} \cdot \nabla) \mathbf{u} = 0 \quad \text{with} \quad \mathbf{v} = \left(\frac{dD_+}{d\tau}\right) \mathbf{u}. \quad (9)$$

Eq.(9) is the equation of motion of free particles, $d\mathbf{u}/dD_+ = 0$, hence the trajectories are given by:

$$\mathbf{x} = \mathbf{q} + D_+(\tau) \mathbf{s}_0(\mathbf{q}), \quad \mathbf{v} = \frac{dD_+}{d\tau} \mathbf{s}_0(\mathbf{q}), \quad (10)$$

where \mathbf{q} is the Lagrangian coordinate and $\mathbf{s} = D_+ \mathbf{s}_0$ is the displacement field. Eq.(10) is the usual definition of the Zeldovich approximation.

Thus, the Zeldovich approximation corresponds to a change of the linear term of the Euler equation, keeping the quadratic term and the continuity equation unchanged. Therefore, the analysis presented in Valageas (2007) for the case of the exact gravitational dynamics applies to the Zeldovich dynamics up to minor modifications. First, the equations of motion (1) and (8) read in Fourier space:

$$\frac{\partial \delta(\mathbf{k}, \tau)}{\partial \tau} + \theta(\mathbf{k}, \tau) = - \int d\mathbf{k}_1 d\mathbf{k}_2 \delta_D(\mathbf{k}_1 + \mathbf{k}_2 - \mathbf{k}) \times \alpha(\mathbf{k}_1, \mathbf{k}_2) \theta(\mathbf{k}_1, \tau) \delta(\mathbf{k}_2, \tau) \quad (11)$$

$$\frac{\partial \theta(\mathbf{k}, \tau)}{\partial \tau} + \left(1 - \frac{3\Omega_m}{2f}\right) \mathcal{H} \theta(\mathbf{k}, \tau) = - \int d\mathbf{k}_1 d\mathbf{k}_2 \delta_D(\mathbf{k}_1 + \mathbf{k}_2 - \mathbf{k}) \beta(\mathbf{k}_1, \mathbf{k}_2) \theta(\mathbf{k}_1, \tau) \theta(\mathbf{k}_2, \tau) \quad (12)$$

where δ_D is the Dirac distribution, the coupling functions α and β are given by:

$$\alpha(\mathbf{k}_1, \mathbf{k}_2) = \frac{(\mathbf{k}_1 + \mathbf{k}_2) \cdot \mathbf{k}_1}{k_1^2}, \quad \beta(\mathbf{k}_1, \mathbf{k}_2) = \frac{|\mathbf{k}_1 + \mathbf{k}_2|^2 (\mathbf{k}_1 \cdot \mathbf{k}_2)}{2k_1^2 k_2^2} \quad (13)$$

and we defined the Fourier transforms as:

$$\delta(\mathbf{k}) = \int \frac{d\mathbf{x}}{(2\pi)^3} e^{-i\mathbf{k} \cdot \mathbf{x}} \delta(\mathbf{x}). \quad (14)$$

As in Crocce & Scoccimarro (2006a,b) let us define the two-component vector ψ as:

$$\psi(\mathbf{k}, \eta) = \begin{pmatrix} \psi_1(\mathbf{k}, \eta) \\ \psi_2(\mathbf{k}, \eta) \end{pmatrix} = \begin{pmatrix} \delta(\mathbf{k}, \eta) \\ -\theta(\mathbf{k}, \eta)/f\mathcal{H} \end{pmatrix}, \quad (15)$$

where we introduced the time coordinate η defined from the linear growing rate D_+ of the density contrast (normalized to unity today):

$$\eta = \ln D_+(\tau) \quad \text{with} \quad D_+(z=0) = 1. \quad (16)$$

Then, the equations of motion (11)-(12) can be written as:

$$\mathcal{O}(x, x') \cdot \psi(x') = K_s(x; x_1, x_2) \cdot \psi(x_1) \psi(x_2), \quad (17)$$

where we introduced the coordinate $x = (\mathbf{k}, \eta, i)$ where $i = 1, 2$ is the discrete index of the two-component vectors. In eq.(17) and in the following we use the convention that repeated coordinates are integrated over as:

$$\mathcal{O}(x, x') \cdot \psi(x') = \int d\mathbf{k}' d\eta' \sum_{i'=1}^2 \mathcal{O}_{i,i'}(\mathbf{k}, \eta; \mathbf{k}', \eta') \psi_{i'}(\mathbf{k}', \eta'). \quad (18)$$

The matrix \mathcal{O} reads:

$$\mathcal{O}(x, x') = \begin{pmatrix} \frac{\partial}{\partial \eta} & -1 \\ 0 & \frac{\partial}{\partial \eta} - 1 \end{pmatrix} \delta_D(\mathbf{k} - \mathbf{k}') \delta_D(\eta - \eta') \quad (19)$$

whereas the symmetric vertex $K_s(x; x_1, x_2) = K_s(x; x_2, x_1)$ writes:

$$K_s(x; x_1, x_2) = \delta_D(\mathbf{k}_1 + \mathbf{k}_2 - \mathbf{k}) \delta_D(\eta_1 - \eta) \delta_D(\eta_2 - \eta) \times \gamma_{i;i_1,i_2}^s(\mathbf{k}_1, \mathbf{k}_2) \quad (20)$$

with:

$$\gamma_{1;1,2}^s(\mathbf{k}_1, \mathbf{k}_2) = \frac{\alpha(\mathbf{k}_2, \mathbf{k}_1)}{2}, \quad \gamma_{1;2,1}^s(\mathbf{k}_1, \mathbf{k}_2) = \frac{\alpha(\mathbf{k}_1, \mathbf{k}_2)}{2}, \quad (21)$$

$$\gamma_{2;2,2}^s(\mathbf{k}_1, \mathbf{k}_2) = \beta(\mathbf{k}_1, \mathbf{k}_2), \quad (22)$$

and zero otherwise (Crocce & Scoccimarro 2006a). We can note that all the dependence on cosmology is contained in the time-redshift relation $\eta \leftrightarrow z$. Indeed, the equation of motion (17) written in terms of the coordinate η no longer involves time-dependent factors such as Ω_m/f^2 . Therefore, the evolution of the density field only depends on cosmology through the time-coordinate $\eta(z)$. In this article we shall study the system defined by the the equation of motion (17), which shows the exact solution (10). This will allow us to compare various expansion methods with exact non-linear results.

2.2. Linear regime

At large scales or at early times where the density and velocity fluctuations are small one can linearize the equation of motion (17) which yields $\mathcal{O}.\psi_L = 0$. This gives the two linear modes:

$$\psi_+ = e^\eta \begin{pmatrix} 1 \\ 1 \end{pmatrix}, \quad \psi_- = \begin{pmatrix} 1 \\ 0 \end{pmatrix}. \quad (23)$$

Of course we recover the linear growing mode ψ_+ of the gravitational dynamics, since the approximation (5) is valid in this case. However, the usual decaying mode ψ_- has been changed to a constant mode. As seen in eq.(23) it corresponds to a mere perturbation of the density field which is transported by the unchanged velocity field. Indeed, since the velocity field is now decoupled from the density field it obeys a first-order differential equation in the linear regime (rather than a second-order differential equation) which only admits one linear mode. As usual we shall define the initial conditions by the linear growing mode ψ_L :

$$\psi_L(x) = e^\eta \delta_{L0}(\mathbf{k}) \begin{pmatrix} 1 \\ 1 \end{pmatrix}, \quad (24)$$

where $\delta_{L0}(\mathbf{k})$ is the linear density contrast today at redshift $z = 0$. In this fashion the system (11)-(12) which we study here agrees with the gravitational dynamics in the linear regime. Besides, from eq.(5) and eq.(10) we see that the displacement field $\mathbf{s}_0(\mathbf{q})$ obeys:

$$\nabla_{\mathbf{q}}.\mathbf{s}_0 = -\delta_{L0}. \quad (25)$$

Moreover, we assume Gaussian homogeneous and isotropic initial conditions defined by the linear power-spectrum $P_{L0}(k)$:

$$\langle \delta_{L0}(\mathbf{k}_1) \delta_{L0}(\mathbf{k}_2) \rangle = \delta_D(\mathbf{k}_1 + \mathbf{k}_2) P_{L0}(k_1). \quad (26)$$

Then, as for the gravitational dynamics studied in Valageas (2007), the linear two-point correlation function $G_L(x_1, x_2)$ reads:

$$\begin{aligned} G_L(x_1, x_2) &= \langle \psi_L(x_1) \psi_L(x_2) \rangle \\ &= \delta_D(\mathbf{k}_1 + \mathbf{k}_2) e^{\eta_1 + \eta_2} P_{L0}(k_1) \begin{pmatrix} 1 & 1 \\ 1 & 1 \end{pmatrix}. \end{aligned} \quad (27)$$

As in Valageas (2004) it is convenient to introduce the response function $R(x_1, x_2)$ (related to the propagator used in Crocce & Scoccimarro (2006a,b), see sect. 3.2.2 below) defined by the functional derivative:

$$R(x_1, x_2) = \left\langle \frac{\delta \psi(x_1)}{\delta \zeta(x_2)} \right\rangle_{\zeta=0}, \quad (28)$$

where $\zeta(x)$ is a ‘‘noise’’ added to the r.h.s. in eq.(17). Thus, $R(x_1, x_2)$ measures the linear response of the system to an external source of noise. Because of causality it contains an Heaviside factor $\theta(\eta_1 - \eta_2)$ since the field $\psi(x_1)$ can only depend on the values of the ‘‘noise’’ at earlier times $\eta_2 \leq \eta_1$. Moreover, it satisfies the initial condition:

$$\eta_1 \rightarrow \eta_2^+ : R(x_1, x_2) \rightarrow \delta_D(\mathbf{k}_1 - \mathbf{k}_2) \delta_{i_1, i_2}. \quad (29)$$

In the linear regime, the response R_L can be obtained from the initial condition (29) and the linear dynamics $\mathcal{O}.R_L = 0$ for $\eta_1 > \eta_2$ (as implied by the definition (28) and $\mathcal{O}.\psi_L = 0$). This yields:

$$\begin{aligned} R_L(x_1, x_2) &= \delta_D(\mathbf{k}_1 - \mathbf{k}_2) \theta(\eta_1 - \eta_2) \\ &\times \left\{ e^{\eta_1 - \eta_2} \begin{pmatrix} 0 & 1 \\ 0 & 1 \end{pmatrix} + \begin{pmatrix} 1 & -1 \\ 0 & 0 \end{pmatrix} \right\}. \end{aligned} \quad (30)$$

This expression holds for any cosmology, whereas for the case of the gravitational dynamics factors such as Ω_m/f^2 lead to a small explicit dependence on cosmological parameters. Note that by symmetry the two-point correlation G has the form:

$$G(x_1, x_2) = \delta_D(\mathbf{k}_1 + \mathbf{k}_2) G_{i_1, i_2}(k_1; \eta_1, \eta_2) \quad (31)$$

with:

$$G_{i_1, i_2}(k; \eta_1, \eta_2) = G_{i_2, i_1}(k; \eta_2, \eta_1) \quad (32)$$

whereas the response function has the form:

$$R(x_1, x_2) = \delta_D(\mathbf{k}_1 - \mathbf{k}_2) \theta(\eta_1 - \eta_2) R_{i_1, i_2}(k_1; \eta_1, \eta_2). \quad (33)$$

On the other hand, as noticed above the linear two-point functions obey:

$$\mathcal{O}(x, z).G_L(z, y) = 0, \quad \mathcal{O}(x, z).R_L(z, y) = \delta_D(x - y). \quad (34)$$

This can also be checked from the explicit expressions (27),(30). Finally, it is convenient to define the power per logarithmic wavenumber $\Delta^2(k)$ by:

$$\Delta^2(k) = 4\pi k^3 P(k), \quad \Delta^2(k; \eta_1, \eta_2) = 4\pi k^3 G_{11}(k; \eta_1, \eta_2) \quad (35)$$

where the second expression generalizes $\Delta^2(k)$ at different times. Note that for $\eta_1 \neq \eta_2$ we can have $\Delta^2(k; \eta_1, \eta_2) < 0$ whereas at equal times we have $\Delta^2(k; \eta, \eta) \geq 0$. Then we have for instance:

$$\langle \delta(\mathbf{x}_1) \delta(\mathbf{x}_2) \rangle = \int_0^\infty \frac{dk}{k} \Delta^2(k) \frac{\sin k|\mathbf{x}_1 - \mathbf{x}_2|}{k|\mathbf{x}_1 - \mathbf{x}_2|}. \quad (36)$$

Thus, for a CDM cosmology the linear power $\Delta_{L0}^2(k)$ grows as k^4 at small k and as $\ln k$ at high k .

3. Path-integral formalism

3.1. Differential form

As in Valageas (2004, 2007) we can apply a path-integral approach to the hydrodynamical system described in sect. 2.1. Let us briefly recall how this can be done from the differential equation (17) (see also Martin et al. 1973; Phythian 1977). In order to include explicitly the initial conditions we rewrite eq.(17) as:

$$\mathcal{O}.\psi = K_s.\psi\psi + \mu_I \quad (37)$$

with $\psi = 0$ for $\eta < \eta_I$ and:

$$\mu_I(x) = \delta_D(\eta - \eta_I) e^{\eta_I} \delta_{L0}(\mathbf{k}) \begin{pmatrix} 1 \\ 1 \end{pmatrix} = \delta_D(\eta - \eta_I) \psi_I(\bar{x}) \quad (38)$$

where we introduced the coordinate \bar{x} :

$$\bar{x} = (\mathbf{k}, i) \quad \text{and} \quad \psi_I(\bar{x}) = \psi_L(\bar{x}, \eta_I) \quad (39)$$

Thus, the source μ_I (which formally plays the role of some external noise) merely provides the initial conditions at time η_I , obtained from the linear growing mode (24). We shall eventually take the limit $\eta_I \rightarrow -\infty$. Next, we define the generating functional $Z[j]$ by:

$$Z[j] = \langle e^{j \cdot \psi} \rangle = \int [d\mu_I] e^{j \cdot \psi[\mu_I] - \frac{1}{2} \mu_I \cdot \Delta_I^{-1} \cdot \mu_I} \quad (40)$$

where we took the average over the Gaussian initial conditions:

$$\langle \mu_I \rangle = 0, \quad \langle \mu_I(x_1) \mu_I(x_2) \rangle = \Delta_I(x_1, x_2), \quad (41)$$

with:

$$\Delta_I(x_1, x_2) = \delta_D(\eta_1 - \eta_I) \delta_D(\eta_2 - \eta_I) G_I(\bar{x}_1, \bar{x}_2), \quad (42)$$

$$G_I(\bar{x}_1, \bar{x}_2) = G_L(\bar{x}_1, \eta_I; \bar{x}_2, \eta_I). \quad (43)$$

All statistical properties of the field ψ may be obtained from $Z[j]$. It is convenient to write eq.(40) as:

$$Z[j] = \int [d\mu_I][d\psi] |\det M| \delta_D(\mu_I - \mathcal{O} \cdot \psi + K_s \cdot \psi) \times e^{j \cdot \psi - \frac{1}{2} \mu_I \cdot \Delta_I^{-1} \cdot \mu_I}, \quad (44)$$

where the Jacobian $|\det M|$ is defined by the functional derivative $M = \delta \mu_I / \delta \psi$. As in Valageas (2007) a simple computation shows that this Jacobian is equal to an irrelevant constant. Then, introducing an imaginary ghost field λ to express the Dirac as an exponential and performing the Gaussian integration over μ_I we obtain:

$$Z[j] = \int [d\psi][d\lambda] e^{j \cdot \psi + \lambda \cdot (-\mathcal{O} \cdot \psi + K_s \cdot \psi) + \frac{1}{2} \lambda \cdot \Delta_I \cdot \lambda}. \quad (45)$$

Thus, the statistical properties of the system (17) are described by the action $S[\psi, \lambda]$ defined by:

$$S[\psi, \lambda] = \lambda \cdot (\mathcal{O} \cdot \psi - K_s \cdot \psi) - \frac{1}{2} \lambda \cdot \Delta_I \cdot \lambda. \quad (46)$$

Moreover, we can note that adding a “noise” ζ to the r.h.s. of eq.(17) amounts to change $\mu_I \rightarrow \mu_I + \zeta$ which translates into $S \rightarrow S - \lambda \cdot \zeta$. Therefore, functional derivatives with respect to ζ are equivalent to insertions of the ghost field λ . In particular, we have:

$$R(x_1, x_2) = \langle \psi(x_1) \lambda(x_2) \rangle, \quad \langle \lambda \rangle = 0, \quad \langle \lambda \lambda \rangle = 0. \quad (47)$$

The response function R is also related to the correlation with the initial conditions μ_I through:

$$\begin{aligned} \langle \psi \mu_I \rangle &= \langle \psi (\mathcal{O} \cdot \psi - K_s \cdot \psi) \rangle \\ &= \int [d\psi][d\lambda] \psi \left[-\frac{\delta}{\delta \lambda} + \Delta_I \cdot \lambda \right] e^{\lambda \cdot (-\mathcal{O} \cdot \psi + K_s \cdot \psi) + \frac{1}{2} \lambda \cdot \Delta_I \cdot \lambda} \\ &= \langle \psi (\Delta_I \cdot \lambda) \rangle = R \cdot \Delta_I \end{aligned} \quad (48)$$

since the integral of a total derivative vanishes and we used the symmetry of Δ_I . This also reads:

$$\langle \psi(x_1) \psi_I(\bar{x}_2) \rangle = R(x_1; \bar{x}, \eta_I) \times G_I(\bar{x}; \bar{x}_2), \quad (49)$$

where we defined the cross-product \times as the dot product (18) without integration over time, such as:

$$R \times \psi_I = \int d\mathbf{k}' \sum_{j=1}^2 R_{ij}(\mathbf{k}, \eta; \mathbf{k}', \eta_I) \psi_{Ij}(\mathbf{k}'). \quad (50)$$

3.2. Integral form

In order to make the connection with the approach developed in Crocce & Scoccimarro (2006a,b) we describe here how the same path-integral method can be applied to the equation of motion (17) written in integral form.

3.2.1. Letting $\eta_I \rightarrow -\infty$

First, as in Valageas (2001) (see also Scoccimarro 2000) we can integrate the equation of motion (17) as:

$$\psi(x) = \psi_L(x) + \tilde{K}_s(x; x_1, x_2) \cdot \psi(x_1) \psi(x_2) \quad (51)$$

with:

$$\mathcal{O} \cdot \tilde{K}_s = K_s \quad \text{or} \quad \tilde{K}_s = R_L \cdot K_s \quad (52)$$

as seen from eq.(34). Here the initial time η_I no longer appears as we have already taken the limit $\eta_I \rightarrow -\infty$. Then, following the same procedure as in sect. 3.1 we can write:

$$Z[j] = \langle e^{j \cdot \psi} \rangle = \int [d\psi_L] e^{j \cdot \psi[\psi_L] - \frac{1}{2} \psi_L \cdot G_L^{-1} \cdot \psi_L}. \quad (53)$$

Introducing again an imaginary field χ to impose the constraint associated with the equation of motion (51) we finally obtain (the Jacobian is equal to unity):

$$Z[j] = \int [d\psi][d\chi] e^{j \cdot \psi + \chi \cdot (-\psi + \tilde{K}_s \cdot \psi) + \frac{1}{2} \chi \cdot G_L \cdot \chi}. \quad (54)$$

Thus, the statistical properties of the system (51) are now described by the action $\mathcal{S}[\psi, \chi]$ defined by:

$$\mathcal{S}[\psi, \chi] = \chi \cdot (\psi - \tilde{K}_s \cdot \psi) - \frac{1}{2} \chi \cdot G_L \cdot \chi. \quad (55)$$

Note that this formulation is equivalent to the one described in sect. 3.1 except that we have already taken the limit $\eta_I \rightarrow -\infty$, directly into the equation of motion (51). From the response field χ we can again obtain a new response function \mathcal{R} associated with eq.(51). From the comparison with eq.(45) we see that we have the relations between both approaches:

$$\chi = \lambda \cdot \mathcal{O}, \quad \mathcal{R} = \langle \psi \chi \rangle = R \cdot \mathcal{O} = \left\langle \frac{\delta \psi}{\delta \psi_L} \right\rangle, \quad (56)$$

where in the last expression we recalled that from eq.(51) a variation with respect to an external noise ζ can be seen as a variation with respect to ψ_L . Note that in the linear regime we simply have $\mathcal{R}_L(x, y) = \delta_D(x - y)$. Moreover, in a fashion similar to eq.(49) we have the property:

$$\begin{aligned} \langle \psi \psi_L \rangle &= \langle \psi (\psi - \tilde{K}_s \cdot \psi) \rangle \\ &= \int [d\psi][d\chi] \psi \left[-\frac{\delta}{\delta \chi} + G_L \cdot \chi \right] e^{\chi \cdot (-\psi + \tilde{K}_s \cdot \psi) + \frac{1}{2} \chi \cdot G_L \cdot \chi} \\ &= \langle \psi (G_L \cdot \chi) \rangle \end{aligned} \quad (57)$$

which yields the relation:

$$\langle \psi(x_1) \psi_L(x_2) \rangle = \mathcal{R}(x_1, x) \cdot G_L(x, x_2) \quad (58)$$

where we used the symmetry of G_L .

3.2.2. Integral form with finite η_I

Finally, as in Crocce & Scoccimarro (2006a,b) it is possible to apply the initial conditions at some finite time η_I , as in sect. 3.1. Thus, we may write the linear growing mode ψ_L at times $\eta > \eta_I$ as:

$$\psi_L(x) = R_L(x; \bar{x}', \eta_I) \times \psi_I(\bar{x}') \quad (59)$$

where ψ_I was defined in eq.(39) and the cross-product \times in eq.(50). Then, following the same procedure as in eqs.(51)- (54), where the Gaussian average is now taken over the field ψ_I with two-point correlation G_I , we now obtain the generating functional:

$$\begin{aligned} Z[j] &= \int [d\psi_I][d\psi][d\chi] e^{j \cdot \psi + \chi \cdot (R_L \times \psi_I - \psi + \tilde{K}_s \cdot \psi \psi) - \frac{1}{2} \psi_I \times G_I^{-1} \times \psi_I} \\ &= \int [d\psi][d\chi] e^{j \cdot \psi + \chi \cdot (-\psi + \tilde{K}_s \cdot \psi \psi) + \frac{1}{2} \chi \cdot (R_L \times G_I \times R_L^T) \cdot \chi} \quad (60) \end{aligned}$$

Of course, we can check that by taking the limit $\eta_I \rightarrow -\infty$ in eq.(60) we recover eq.(54) since we have:

$$\eta_1, \eta_2 > \eta_I: G_L(\eta_1, \eta_2) = R_L(\eta_1, \eta_I) \times G_I \times R_L^T(\eta_2, \eta_I). \quad (61)$$

The system is now described by the action $\tilde{\mathcal{S}}[\psi, \chi]$ defined by:

$$\tilde{\mathcal{S}}[\psi, \chi] = \chi \cdot (\psi - \tilde{K}_s \cdot \psi \psi) - \frac{1}{2} \chi \cdot (R_L \times G_I \times R_L^T) \cdot \chi. \quad (62)$$

Next, we can define a response function with respect to the initial conditions by:

$$\tilde{\mathcal{R}}(x_1, \bar{x}_2) = \left\langle \frac{\delta \psi(x_1)}{\delta \psi_I(\bar{x}_2)} \right\rangle = \langle \psi(x_1) \chi(x) \cdot R_L(x; \bar{x}_2, \eta_I) \rangle. \quad (63)$$

From the comparison of (62) with (46) we obtain $\chi = \lambda \cdot \mathcal{O}$ and:

$$\tilde{\mathcal{R}}(x_1, \bar{x}_2) = R \cdot \mathcal{O} \cdot R_L = R(x_1; \bar{x}_2, \eta_I). \quad (64)$$

Thus, the response $\tilde{\mathcal{R}}(x_1, \bar{x}_2)$, which is called the ‘‘propagator $G_{i_1 i_2}(k_1, \eta_1) \delta_D(\mathbf{k}_1 - \mathbf{k}_2)$ ’’ in Crocce & Scoccimarro (2006a,b) is equal to the response function R of sect. 3.1 restricted to time $\eta_2 = \eta_I$, without taking the limit $\eta_I \rightarrow -\infty$. Finally, we can note that from eq.(49) we have:

$$\langle \psi(x_1) \psi_I(\bar{x}_2) \rangle = \tilde{\mathcal{R}}(x_1; \bar{x}) \times G_I(\bar{x}, \bar{x}_2). \quad (65)$$

This relation was obtained in Crocce & Scoccimarro (2006b) from a diagrammatic approach. Thus, we see that the three approaches (46), (55) and (62) are closely related. In the integral method we simply absorb the matrix \mathcal{O} into the response field χ . Besides, we can either take the limit $\eta_I \rightarrow -\infty$ from the start, as for the action \mathcal{S} , or keep a finite η_I in the computation as for $\tilde{\mathcal{S}}$. Then, we can take $\eta_I \rightarrow -\infty$ in the final results for the non-linear two-point

correlation. Note however that for the approach of Crocce & Scoccimarro (2006a,b), which corresponds to the action $\tilde{\mathcal{S}}$, it is not possible to take this limit in a practical manner, since one needs to keep track of the response $\tilde{\mathcal{R}}$ which has no finite limit for $\eta_I \rightarrow -\infty$. This leads to somewhat more complicated expressions than for the approaches based on the actions \mathcal{S} and \mathcal{S} of eqs.(46),(55) where the response functions R and \mathcal{R} remain well-defined for $\eta_I \rightarrow -\infty$. Of course, the analysis described above also applies to the case of the gravitational dynamics.

4. Large- N expansions

The path-integrals (45), (54) and (60) can be computed by expanding over powers of the non-Gaussian part (i.e. over powers of K_s or \tilde{K}_s). This actually gives the usual perturbative expansion over powers of the linear power-spectrum P_L (see also Valageas (2001, 2004) for the case of the Vlasov equation of motion). On the other hand, these path-integrals may also be studied through large- N expansions as in Valageas (2004). We focus below on the differential form (45) but the formalism also applies to the integral forms (54) and (60). Thus, one considers the generating functional $Z_N[j, h]$ defined by:

$$Z_N[j, h] = \int [d\psi][d\lambda] e^{N[j \cdot \psi + h \cdot \lambda - \mathcal{S}[\psi, \lambda]]} \quad (66)$$

and one looks for an expansion over powers of $1/N$, taking eventually $N = 1$ into the results. As discussed in Valageas (2004) the large- N expansions may also be derived from a generalization of the dynamics to N fields $\psi^{(\alpha)}$. This yields the same results once we take care of the long-wavelength divergences which constrain which subsets of diagrams need to be gathered. We shall discuss below both ‘‘linear schemes’’, such as the standard perturbation theory or the steepest-descent method of sect. 4.1, which involve expansions over linear two-point functions, and ‘‘non-linear schemes’’, such as the 2PI effective action method of sect. 4.2, which involve expansions over non-linear two-point functions themselves. By expanding different intermediate quantities or different equations (derived from the same equation of motion) one obtains different methods which also correspond to different partial resummations.

4.1. Steepest-descent method

A first approach to handle the large- N limit of eq.(66) is to use a steepest-descent method (also called a semi-classical or loopwise expansion in the case of usual Quantum field theory with $\hbar = 1/N$). This yields for auxiliary correlation and response functions G_0 and R_0 the equations (Valageas 2004):

$$\mathcal{O}(x, z) \cdot G_0(z, y) = 0 \quad (67)$$

$$\mathcal{O}(x, z) \cdot R_0(z, y) = \delta_D(x - y) \quad (68)$$

$$R_0(x, z) \cdot \mathcal{O}(z, y) = \delta_D(x - y) \quad (69)$$

whereas the actual correlation and response functions obey:

$$\mathcal{O}(x, z).G(z, y) = \Sigma(x, z).G(z, y) + \Pi(x, z).R^T(z, y) \quad (70)$$

$$\mathcal{O}(x, z).R(z, y) = \delta_D(x - y) + \Sigma(x, z).R(z, y) \quad (71)$$

$$R(x, z).\mathcal{O}(z, y) = \delta_D(x - y) + R(x, z).\Sigma(z, y) \quad (72)$$

where the self-energy terms Σ and Π are given at one-loop order by:

$$\Sigma(x, y) = 4K_s(x; x_1, x_2)K_s(z; y, z_2)R_0(x_1, z)G_0(x_2, z_2) \quad (73)$$

$$\Pi(x, y) = 2K_s(x; x_1, x_2)K_s(y; y_1, y_2)G_0(x_1, y_1)G_0(x_2, y_2) \quad (74)$$

Note that eqs.(67)-(72) are exact and that the expansion over powers of $1/N$ only enters the expression of the self-energy (73)-(74). Here we only kept the lowest-order terms (see Valageas (2004) for the next-order terms). We also took the limit $\eta_I \rightarrow -\infty$ so that terms involving Δ_I vanish. The comparison of eqs.(67)-(68) with eqs.(34) shows that the auxiliary matrices G_0 and R_0 are actually equal to their linear counterparts:

$$G_0 = G_L, \quad R_0 = R_L. \quad (75)$$

Next, substituting G_0 and R_0 into eqs.(73)-(74) we obtain the self-energies at one-loop order. First, we can note that Σ has the same form (33) as the response R whereas Π is symmetric and has the same form (31) as the two-point correlation G . Then, a simple calculation gives:

$$\Sigma_0(x_1, x_2) = -\omega_1^2 \theta(\eta_1 - \eta_2) \delta_D(\mathbf{k}_1 - \mathbf{k}_2) \times \left[e^{2\eta_1} \begin{pmatrix} 0 & 1 \\ 0 & 1 \end{pmatrix} + e^{\eta_1 + \eta_2} \begin{pmatrix} 1 & -1 \\ 0 & 0 \end{pmatrix} \right], \quad (76)$$

where we defined $\omega_1 = \omega(k_1)$ as:

$$\omega(k) = k\sigma_v, \quad \text{with } \sigma_v^2 = \frac{1}{3} \langle s_0^2 \rangle = \frac{4\pi}{3} \int_0^\infty dw P_{L0}(w). \quad (77)$$

Here σ_v^2 is the variance of the one-dimensional displacement field \mathbf{s} (or of the one-dimensional velocity dispersion up to a normalization factor). On the other hand, Π is given at one-loop order by:

$$\Pi_0(x_1, x_2) = \delta_D(\mathbf{k}_1 + \mathbf{k}_2) e^{2\eta_1 + 2\eta_2} \Pi_0(k_1), \quad (78)$$

with:

$$\Pi_0(k) = 2 \int d\mathbf{k}_1 d\mathbf{k}_2 \delta_D(\mathbf{k}_1 + \mathbf{k}_2 - \mathbf{k}) P_{L0}(k_1) P_{L0}(k_2) \times \begin{pmatrix} \pi_1^2 & \pi_1 \pi_2 \\ \pi_1 \pi_2 & \pi_2^2 \end{pmatrix} \quad (79)$$

and:

$$\pi_1 = \frac{\mathbf{k} \cdot \mathbf{k}_1}{2k_1^2} + \frac{\mathbf{k} \cdot \mathbf{k}_2}{2k_2^2}, \quad \pi_2 = \frac{k^2(\mathbf{k}_1 \cdot \mathbf{k}_2)}{2k_1^2 k_2^2}. \quad (80)$$

Then, the response R and the correlation G can be obtained by integrating eqs.(70)-(71).

4.2. 2PI effective action method

As described in Valageas (2004) a second approach is to first introduce the double Legendre transform $\Gamma[\psi, G]$ of the functional $W = \ln Z$ (with respect to both the field ψ and its two-point correlation G) and next to apply the $1/N$ expansion to Γ . This ‘‘2PI effective action’’ method yields the same equations (70)-(72) and the self-energy shows the same structure at one-loop order as (73)-(74) where G_0 and R_0 are replaced by G and R :

$$\Sigma(x, y) = 4K_s(x; x_1, x_2)K_s(z; y, z_2)R(x_1, z)G(x_2, z_2) \quad (81)$$

$$\Pi(x, y) = 2K_s(x; x_1, x_2)K_s(y; y_1, y_2)G(x_1, y_1)G(x_2, y_2) \quad (82)$$

Thus, the direct steepest-descent method yields a series of linear equations which can be solved directly whereas the 2PI effective action method gives a system of non-linear equations (through the dependence on G and R of Σ and Π) which must usually be solved numerically by an iterative scheme. However, thanks to the Heaviside factors appearing in the response R and the self-energy Σ these equations can be solved directly by integrating forward over time η_1 .

4.3. Role of self-energy terms

From eq.(71) we can see that the self-energy Σ plays the role of a damping term. Indeed, eq.(71) is of the form $\partial R / \partial \eta_1 = \Sigma.R$ so that large negative values of Σ are associated with a strong damping of the response function (exact details are somewhat more intricate since eq.(71) is actually an integro-differential equation). This agrees with eq.(76) which shows that the one-loop self-energy Σ_0 becomes large and negative at high k as $\Sigma_0 \propto -k^2$. Thus, the self-energy Σ encodes the loss of memory associated with the small-scale non-linear dynamics.

On the other hand, from eq.(70) we can see that the self-energy Π is associated with the continuous production of power due to non-linear mode couplings. Indeed, from eqs.(70)-(72) we can see that the correlation G can also be written in terms of the response R as:

$$G(x_1, x_2) = R \times G_I \times R^T + R.\Pi.R^T \quad (83)$$

and we let $\eta_I \rightarrow -\infty$. The physical meaning of eq.(83) is clear. The first term in the r.h.s. means that the fluctuations at the initial time η_I are merely transported forward in time through the response R . This is the only non-zero term in the linear regime (with $R = R_L$ and $G_0 = G_L$). The effect of the non-linear dynamics is to modify the transport matrix R and to add a second term to the r.h.s. of eq.(83). The latter has the meaning of a source term which produces fluctuations with two-point correlation $\Pi(\eta'_1, \eta'_2)$ at the times (η'_1, η'_2) which are next transported forward to later times (η_1, η_2) by the matrices $R(\eta_1, \eta'_1)$ and $R^T(\eta'_2, \eta_2)$.

5. Running with a high- k cutoff

In a recent paper, Matarrese & Pietroni (2007) introduced another approach to study the gravitational dynamics

within the hydrodynamical framework which is also based on a path-integral formulation. Although they used the integral form of the equations of motion, as in sect. 3.2, we briefly describe in this section how this method may be applied to the path-integral (45). First, from eq.(45) we define the generating functional $Z[j, h]$ as:

$$Z[j, h] = \int [d\psi][d\lambda] e^{j \cdot \psi + h \cdot \lambda - S[\psi, \lambda]}, \quad (84)$$

where we have introduced the external source h . This allows one to obtain the correlations of the response field λ through derivatives with respect to h . Next, following Matarrese & Pietroni (2007) we add a high- k cutoff Λ to the linear power-spectrum $P_{L0}(k)$ by changing the kernel Δ_I which appears in the action S of eq.(46) as:

$$\Delta_I \rightarrow \Delta_\Lambda = \theta(\Lambda - k_1) \Delta_I(x_1, x_2). \quad (85)$$

Thus, the Heaviside factor $\theta(\Lambda - k_1)$ removes the linear power at high wavenumbers $k_1 > \Lambda$ and we recover the full system in the limit $\Lambda \rightarrow \infty$. Then, the idea proposed in Matarrese & Pietroni (2007) is to study the evolution of the system as a function of the cutoff Λ . Therefore, one first looks for equations which describe the dependence on Λ . Second, one derives some approximation for these equations, for instance by a truncation of some expansion, and finally one solves these approximate equations from $\Lambda = 0$ up to $\Lambda = \infty$. First, the dependence on Λ may obviously be described through the derivative of Z with respect to Λ which reads:

$$\frac{\partial Z}{\partial \Lambda} = \frac{e^{2\eta_I} P_{L0}(\Lambda)}{2} \int d\mathbf{k} \delta_D(\Lambda - k) \sum_{i,j} \frac{\delta^2 Z}{\delta h_i(\mathbf{k}, \eta_I) \delta h_j(-\mathbf{k}, \eta_I)} \quad (86)$$

Next, introducing the generating functional W of the connected correlation functions:

$$W = \ln Z, \quad R(x_1, x_2) = \left. \frac{\delta^2 W}{\delta j(x_1) \delta h(x_2)} \right|_{j=h=0}, \quad (87)$$

we obtain from eq.(86) the evolution of the response R with the cutoff Λ as:

$$\frac{\partial R}{\partial \Lambda}(x_1, x_2) = \frac{e^{2\eta_I} P_{L0}(\Lambda)}{2} \int d\mathbf{w} \delta_D(\Lambda - w) \times \sum_{i,j} \frac{\delta^4 W}{\delta h_i(\mathbf{w}, \eta_I) \delta h_j(-\mathbf{w}, \eta_I) \delta j(x_1) \delta h(x_2)}. \quad (88)$$

Here we used the property (47): $\langle \lambda \rangle = \langle \lambda \lambda \rangle = 0$. Next, in order to make some progress one needs to obtain an expression for the fourth-derivative $W^{(4)}$. Of course, in generic cases this quantity is not known exactly and one must introduce some approximations. The usual procedure is to write a diagrammatic expansion for W , using the path-integral expression (84), and to truncate at some finite order. For the cubic action (46), the lowest-order contribution is associated with the diagram of Fig. 1 which gives:

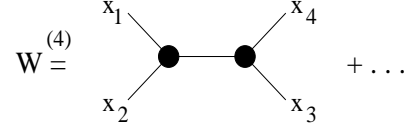


Fig. 1. The first diagram of the expansion of the fourth derivative $W^{(4)}$ as in eq.(89). The big dots are the vertices K_s and the lines are the two-point functions R or G .

$$\begin{aligned} \frac{\delta^4 W}{\delta j_1 \delta h_2 \delta h_3 \delta h_4} &= \langle \psi_1 \lambda_2 \lambda_3 \lambda_4 \rangle_c \\ &= 12RR(K_s RK_s)RR + \dots \end{aligned} \quad (89)$$

Using the expression (20) of the vertex K_s this gives:

$$\begin{aligned} \frac{\partial R_{i_1 i_2}}{\partial \Lambda}(k; \eta_1, \eta_2) &= 4e^{2\eta_I} P_{L0}(\Lambda) \int d\mathbf{w} \delta_D(\Lambda - w) \int_{\eta_2}^{\eta_1} d\eta \int_{\eta_2}^{\eta} d\eta' \\ &\times R_{i_1 i'_1}(k; \eta_1, \eta) R_{i'_2 i_2}(k; \eta', \eta_2) R_{i'_3 i_3}(w; \eta, \eta_I) R_{i'_4 i_4}(w; \eta', \eta_I) \\ &\times R_{ij}(\mathbf{k} - \mathbf{w}; \eta, \eta') \gamma_{i'_1 i'_3 i}^s(\mathbf{w}, \mathbf{k} - \mathbf{w}) \gamma_{j i'_2 i'_4}^s(\mathbf{k}, -\mathbf{w}) \end{aligned} \quad (90)$$

Following Matarrese & Pietroni (2007), we note that at lowest-order we may replace the response functions in the r.h.s. in eq.(90) by the linear responses, which do not depend on Λ since they do not depend on the linear power-spectrum, see eq.(30). Then, in the limit $\eta_I \rightarrow -\infty$ only the linear growing modes of $R_{i'_3 i_3}$ and $R_{i'_4 i_4}$ give a non-vanishing contribution:

$$\begin{aligned} \frac{\partial R_{i_1 i_2}}{\partial \Lambda} &= 4P_{L0}(\Lambda) \int d\mathbf{w} \delta_D(\Lambda - w) \int_{\eta_2}^{\eta_1} d\eta \int_{\eta_2}^{\eta} d\eta' e^{\eta + \eta'} \\ &\times R_{L i_1 i'_1}(\eta_1, \eta) R_{L i'_2 i_2}(\eta', \eta_2) R_{L ij}(\eta, \eta') \\ &\times \gamma_{i'_1 i'_3 i}^s(\mathbf{w}, \mathbf{k} - \mathbf{w}) \gamma_{j i'_2 i'_4}^s(\mathbf{k}, -\mathbf{w}). \end{aligned} \quad (91)$$

Next, using eqs.(21)-(22) for the vertices γ^s we obtain:

$$\frac{\partial R}{\partial \Lambda} = -\frac{4\pi}{3} k^2 P_{L0}(\Lambda) \frac{(D_1 - D_2)^2}{2} R_L. \quad (92)$$

Starting from the initial condition $R(\Lambda = 0) = R_L$ this yields at $\Lambda = \infty$:

$$R = R_L \left[1 - \frac{\omega^2 (D_1 - D_2)^2}{2} \right], \quad (93)$$

which agrees with the usual perturbative result at order P_{L0} (see eq.(155) below). Next, the running with Λ of the two-point correlation G (whence of the non-linear power-spectrum) is obtained by taking the derivative with respect to Λ of eq.(83) and using again a loopwise expansion for the self-energy Π . In practice, Matarrese & Pietroni (2007) use some ansatz for G to derive a linear equation which can be solved up to $\Lambda = \infty$. Although they refer to this approach as a renormalization group method we can note that it is somewhat different from the usual renormalization group techniques. Indeed, although one considers the evolution with a cutoff Λ one does not look for a fixed point of renormalization group equations which

would govern the properties of the system in some large-scale limit.

Matarrese & Pietroni (2007) noticed that if we promote the linear response R_L in the r.h.s. of eq.(92) to the non-linear response R we obtain as the solution of this linear equation the response (133) with a Gaussian decay at high k . For the Zeldovich dynamics this happens to be the exact non-linear response function. Note that all the previous steps apply identically to the case of the gravitational dynamics, where this procedure leads again to the response (133). In this case, this expression is no longer exact but it shows the expected damping into the non-linear regime. This remark suggests that this procedure may provide a very efficient expansion scheme for the response function. However, this is somewhat artificial. Indeed, in order to derive eq.(92) from eq.(90) one made use of the properties of the linear response to simplify the r.h.s. so that substituting back the non-linear response R is somewhat ad-hoc (although it is correct at lowest-order it makes the procedure not systematic). Moreover, it is clear that one can apply the same procedure to any other scheme which gives an equation of the form $\partial R/\partial\alpha = F[P_{L0}, R, G]$ where α can be any variable among $\{k, \eta_1, \eta_2, \Lambda, \dots\}$ (for the large- N expansions of sect. 4 it would be η_1). Indeed, at lowest order one can always simplify F as a linear functional of R_L such that by substituting $R_L \rightarrow R$ one obtains the exact response (133), since the r.h.s. must be consistent at lowest-order with $\partial R/\partial\alpha$ evaluated for the exact response (133). Thus, the latter satisfies the equation:

$$\frac{\partial R}{\partial\alpha} = \left[\frac{\partial \ln R_L}{\partial\alpha} - \frac{1}{2} \frac{\partial}{\partial\alpha} (D_1 - D_2)^2 \omega^2 \right] R, \quad (94)$$

which implies that at lowest order one can always write $\partial R/\partial\alpha = F[P_{L0}, R, G]$ as:

$$\left[\frac{\partial}{\partial\alpha} - \frac{\partial \ln R_L}{\partial\alpha} \right] R = -\frac{1}{2} \left(\frac{\partial}{\partial\alpha} (D_1 - D_2)^2 \omega^2 \right) R_L + \dots \quad (95)$$

where the dots stand for higher-order terms over $\{(D_1 - D_2), \omega\}$. For the specific case $\alpha = \Lambda$ eq.(95) gives back eq.(92). For the large- N expansion schemes eq.(95) would be eq.(71) with $\alpha \rightarrow \eta_1$, the l.h.s. corresponding to $\mathcal{O}.R$ and the r.h.s. to $\Sigma.R$ at lowest-order. Then, substituting R to R_L in the r.h.s. of eq.(95) one recovers eq.(94) and the non-linear response (133) with the Gaussian cutoff. This reasoning also applies to the gravitational dynamics to which one adds high- k approximations so that the response (133) (or a variant) still applies, see also sect. 9 below. Therefore, recovering the response (133) in this manner does not imply that the underlying expansion scheme is very efficient. We shall discuss this method, based on the dependence of the system on a high- k cutoff Λ , in sect. 12 below within the framework of a simple systematic expansion and we shall find that it actually gives similar results as the 2PI effective action method.

6. Exact two-point functions

For the Zeldovich dynamics all quantities of interest can be computed exactly since we know the solution (10) of the equations of motion. This makes the Zeldovich dynamics an interesting test for approximation schemes since we can compare their predictions with exact result. As the equations of motion in the form (11)-(12) are very similar to those associated with the exact gravitational dynamics, we can expect that the behavior of various approximation schemes will be similar for both dynamics. Therefore, we compute in this section the exact two-point functions associated with the Zeldovich dynamics.

6.1. Two-point correlation

As is well known, for the Zeldovich dynamics the two-point correlation G can be computed exactly from the solution (10) of the equations of motion (e.g. Schneider & Bartelmann 1995; Taylor & Hamilton 1996). Indeed, starting from the uniform density $\bar{\rho}$ at $t \rightarrow 0$ the conservation of matter gives before orbit-crossing:

$$\rho(\mathbf{x})d\mathbf{x} = \bar{\rho}d\mathbf{q} \quad \text{whence} \quad 1 + \delta(\mathbf{x}) = \left[\det \left(\frac{\partial \mathbf{x}}{\partial \mathbf{q}} \right) \right]^{-1}. \quad (96)$$

This also reads from eq.(10):

$$\delta(\mathbf{x}, \eta) = \int d\mathbf{q} \delta_D[\mathbf{x} - \mathbf{q} - \mathbf{s}(\mathbf{q}, \eta)] - 1, \quad (97)$$

where $\mathbf{s}(\mathbf{q}, \eta) = D_+(\eta)\mathbf{s}_0(\mathbf{q})$ is the displacement field. We can note that this expression remains valid after shell-crossing: all particles of Lagrangian coordinate \mathbf{q} which happen to be at location \mathbf{x} at the time of interest contribute to the r.h.s. In Fourier space we obtain for $k \neq 0$:

$$\delta(\mathbf{k}) = \int \frac{d\mathbf{q}}{(2\pi)^3} e^{-i\mathbf{k}\cdot(\mathbf{q}+\mathbf{s})}. \quad (98)$$

Therefore, the density-density two-point correlation reads:

$$\delta_D(\mathbf{k}_1 + \mathbf{k}_2)G_{11}(k_1; \eta_1, \eta_2) = \int \frac{d\mathbf{q}_1 d\mathbf{q}_2}{(2\pi)^6} e^{-i(\mathbf{k}_1 \cdot \mathbf{q}_1 + \mathbf{k}_2 \cdot \mathbf{q}_2)} \langle e^{-i(\mathbf{k}_1 \cdot \mathbf{s}_1 + \mathbf{k}_2 \cdot \mathbf{s}_2)} \rangle. \quad (99)$$

Since the displacement field \mathbf{s}_0 given by eq.(25) is Gaussian the average in eq.(99) reads:

$$\langle e^{-i(\mathbf{k}_1 \cdot \mathbf{s}_1 + \mathbf{k}_2 \cdot \mathbf{s}_2)} \rangle = e^{-\frac{1}{2} \langle (k_{1i} s_{1i} + k_{2i} s_{2i})(k_{1j} s_{1j} + k_{2j} s_{2j}) \rangle}, \quad (100)$$

where we sum over the 3D components $i, j = 1, 2, 3$. Let us define the displacement correlation Ψ_0 :

$$\Psi_{0;ij}(\mathbf{q}_1, \mathbf{q}_2) = \langle s_{0;i}(\mathbf{q}_1) s_{0;j}(\mathbf{q}_2) \rangle. \quad (101)$$

Thanks to statistical homogeneity it obeys:

$$\Psi_{0;ij}(\mathbf{q}_1, \mathbf{q}_2) = \Psi_{0;ij}(\mathbf{q}_1 - \mathbf{q}_2) \quad (102)$$

and from eq.(25) it is given by:

$$\Psi_{0;ij}(\mathbf{q}) = \int d\mathbf{k} e^{i\mathbf{k}\cdot\mathbf{q}} \frac{k_i k_j}{k^4} P_{L0}(k). \quad (103)$$

Then, eq.(99) writes:

$$G_{11}(k; \eta_1, \eta_2) = \int \frac{d\mathbf{q}}{(2\pi)^3} e^{-i\mathbf{k}\cdot\mathbf{q}} \times e^{e^{\eta_1+\eta_2} k_i k_j [\Psi_{0;ij}(\mathbf{q}) - \cosh(\eta_1 - \eta_2) \Psi_{0;ij}(0)]}. \quad (104)$$

Using eq.(103) this can also be written as:

$$G_{11}(k; \eta_1, \eta_2) = \int \frac{d\mathbf{q}}{(2\pi)^3} e^{-i\mathbf{k}\cdot\mathbf{q}} \times e^{e^{\eta_1+\eta_2} \int d\mathbf{w} \frac{(\mathbf{k}\cdot\mathbf{w})^2}{w^4} P_{L0}(w) [\cos(\mathbf{w}\cdot\mathbf{q}) - \cosh(\eta_1 - \eta_2)]}. \quad (105)$$

The integration over angles in the exponent of eq.(105) can be performed analytically. Thus, let us define the quantity $I(\mathbf{q}; \mathbf{k})$ by:

$$I(\mathbf{q}; \mathbf{k}) = k_i k_j \Psi_{0;ij}(\mathbf{q}) = \int d\mathbf{w} e^{i\mathbf{w}\cdot\mathbf{q}} \frac{(\mathbf{k}\cdot\mathbf{w})^2}{w^4} P_{L0}(w). \quad (106)$$

Then, by expanding the exponential over spherical harmonics we obtain:

$$I(\mathbf{q}; \mathbf{k}) = k^2 I_0(q) + k^2 (1 - 3\mu^2) I_2(q), \quad \mu = \frac{\mathbf{k}\cdot\mathbf{q}}{kq}, \quad (107)$$

where we introduced:

$$I_n(q) = \frac{4\pi}{3} \int_0^\infty dw P_{L0}(w) j_n(wq) \quad (108)$$

and j_n is the spherical Bessel function of order n . Note that the variance σ_v^2 of the one-dimensional displacement field, defined in eq.(77), also satisfies $\sigma_v^2 = I_0(0)$. Then, eq.(105) reads (using the linear growth factor $D = e^\eta$ as the time-coordinate):

$$G_{11}(k; D_1, D_2) = e^{-\frac{D_1^2+D_2^2}{2} k^2 \sigma_v^2} \int \frac{d\mathbf{q}}{(2\pi)^3} \cos(kq\mu) \times e^{D_1 D_2 k^2 [I_0 + (1-3\mu^2) I_2]}. \quad (109)$$

Following Schneider & Bartelmann (1995) we can perform the integration over angles by expanding the exponential and using the property:

$$\int_0^1 d\mu \cos(kq\mu) (1 - \mu^2)^n = n! \left(\frac{2}{kq}\right)^n j_n(kq). \quad (110)$$

This gives:

$$G_{11}(k; D_1, D_2) = e^{-\frac{D_1^2+D_2^2}{2} k^2 \sigma_v^2} \int_0^\infty \frac{dq q^2}{2\pi^2} e^{D_1 D_2 k^2 (I_0 - 2I_2)} \times \sum_{n=0}^\infty \left(D_1 D_2 \frac{6k^2 I_2}{kq} \right)^n j_n(kq). \quad (111)$$

6.2. Asymptotic behavior

From the explicit expression (109) we can obtain the asymptotic behavior of the two-point correlation function in the highly non-linear regime. Thus, we can write formally for a power-law linear power spectrum:

$$G_{11} = e^{[D_1 D_2 - \frac{D_1^2+D_2^2}{2}] k^2 \sigma_v^2} \frac{1}{4\pi k^3} F[\Delta_L^2(k; D_1, D_2)] \quad (112)$$

with:

$$F(x) = \int \frac{dq}{2\pi^2} \cos(q\mu) e^{\frac{x}{3} \int dw w^n [j_0(qw) - 1 + (1-3\mu^2) j_2(qw)]} \quad (113)$$

where we made the change of variables $q \rightarrow q/k$, $w \rightarrow kw$, for:

$$P_{L0}(k) = \frac{1}{4\pi k_0^3} \left(\frac{k}{k_0}\right)^n, \quad (114)$$

whence:

$$\Delta_L^2(k; D_1, D_2) = D_1 D_2 \left(\frac{k}{k_0}\right)^{n+3}. \quad (115)$$

First, we can note that infrared (IR) divergences appear in the one-dimensional velocity dispersion σ_v^2 , defined in eq.(77), for $n \leq -1$ at low k , and in the integral over w in eq.(113) for $n \leq -3$. As is well-known, the IR divergence at $n \leq -1$ should disappear for equal-time statistics (Vishniac 1983; Jain & Bertschinger 1996) because of Galilean invariance. This is explicitly checked in eq.(112) since for $D_1 = D_2$ the prefactor of $k^2 \sigma^2$ vanishes so that the contribution associated with σ_v cancels out. Thus the equal-time non-linear power spectrum is well-defined for $n > -3$. Second, we can see that both σ_v^2 and the integral over w in eq.(113) diverge if $n \geq -1$ at high k . Thus, this UV divergence remains untamed in the full non-perturbative result (112). This is a qualitative difference with the true gravitational dynamics where such UV divergences are expected to disappear in the exact non-linear power-spectrum for $-3 < n < 1$. However, this may require to go beyond the single-stream approximation. Therefore, in the following we assume $-3 < n < -1$. After performing the integral over w and making a change of variable we obtain:

$$F(x) = x^{\frac{3}{n+1}} \frac{2}{\pi} \int_0^\infty dq q^2 \int_0^1 d\mu \cos\left(x^{\frac{1}{n+1}} q\mu\right) \times \exp\left[-q^{-n-1} \frac{\pi^{1/2} 2^{n-1} \Gamma[(n+3)/2]}{(-n-1)\Gamma[(4-n)/2]} [1 - (n+1)\mu^2]\right] \quad (116)$$

which shows that $F(x)$ is well-defined for $-3 < n < -1$ and obeys the asymptotic behavior:

$$F(x) \sim x^{\frac{3}{n+1}} \quad \text{for } x \gg 1. \quad (117)$$

Thus, the equal-time power $\Delta^2(k; D)$ decreases in the highly non-linear regime as:

$$\Delta^2(k; D) \sim \Delta_L^2(k; D)^{\frac{3}{n+1}} \quad \text{for } \Delta_L^2 \gg 1. \quad (118)$$

Therefore, if $P_{L0}(k) \sim k^n$ at high k the non-linear power decreases as a power-law $P(k) \sim k^{-3+3(n+3)/(n+1)}$ in the highly non-linear regime.

6.3. Response function

Using the exact solution (10) we can compute the exact response function R . First, we can note that since

the velocity field is decoupled from the density field we have the simple exact result:

$$R_{21} = 0. \quad (119)$$

Of course, the linear solution (30) is consistent with eq.(119). Next, we can compute the response R_{12} of the density to a velocity perturbation as follows. At time η_2^- , before the velocity perturbation localized at time η_2 , the location and velocity of the particle of Lagrangian coordinate \mathbf{q} are from eq.(10):

$$\mathbf{x}_2^- = \mathbf{q} + D_2 \mathbf{s}_0(\mathbf{q}), \quad \mathbf{v}_2^- = \dot{D}_2 \mathbf{s}_0(\mathbf{q}) \quad (120)$$

whereas at time η_2^+ , after the velocity perturbation $\zeta_2(\mathbf{x})$, we have:

$$\mathbf{x}_2^+ = \mathbf{x}_2^-, \quad \mathbf{v}_2^+ = \mathbf{v}_2^- - f_2 \mathcal{H}_2 \nabla_{\mathbf{x}_2}^{-1} \cdot \zeta_2 \quad (121)$$

where we used the definition of ψ_2 in eq.(15). Therefore, the location of the particle at time $\eta_1 > \eta_2$ is:

$$\mathbf{x}_1 = \mathbf{q} + D_1 \mathbf{s}_0(\mathbf{q}) - \frac{D_1 - D_2}{D_2} \nabla_{\mathbf{x}_2}^{-1} \cdot \zeta_2 \quad (122)$$

The density contrast is again given by expressions of the form (96)-(98) so that $\psi_1(\mathbf{k}_1, \eta_1) = \delta(\mathbf{k}_1, \eta_1)$ reads for $k_1 \neq 0$:

$$\psi_1(\mathbf{k}_1, \eta_1) = \int \frac{d\mathbf{q}}{(2\pi)^3} e^{-i\mathbf{k}_1 \cdot [\mathbf{q} + D_1 \mathbf{s}_0 - \frac{D_1 - D_2}{D_2} \nabla_{\mathbf{x}_2}^{-1} \cdot \zeta_2]}. \quad (123)$$

The definition (28) of the response function reads here:

$$R_{12}(\mathbf{k}_1, \eta_1; \mathbf{k}_2, \eta_2) = \left\langle \frac{\delta\psi_1(\mathbf{k}_1)}{\delta\zeta_2(\mathbf{k}_2)} \Big|_{\zeta_2=0} \right\rangle. \quad (124)$$

Then, using the expression:

$$-\nabla_{\mathbf{x}_2}^{-1} \cdot \zeta_2 = \int d\mathbf{k} e^{i\mathbf{k} \cdot \mathbf{x}_2} i \frac{\mathbf{k}}{k^2} \zeta_2(\mathbf{k}) \quad (125)$$

we obtain from eq.(123):

$$R_{12} = \frac{D_1 - D_2}{D_2} \frac{\mathbf{k}_1 \cdot \mathbf{k}_2}{k_2^2} \int \frac{d\mathbf{q}}{(2\pi)^3} e^{i(\mathbf{k}_2 - \mathbf{k}_1) \cdot \mathbf{q}} \times \langle e^{-i(D_1 \mathbf{k}_1 - D_2 \mathbf{k}_2) \cdot \mathbf{s}_0(\mathbf{q})} \rangle. \quad (126)$$

Because of homogeneity the average in eq.(126) does not depend on \mathbf{q} so that the integral over \mathbf{q} yields a Dirac factor $\delta_D(\mathbf{k}_1 - \mathbf{k}_2)$. On the other hand, since \mathbf{s}_0 is Gaussian the average can be easily performed as in sect. 6.1 and this gives for $D_1 > D_2$:

$$R_{12}(k; D_1, D_2) = \frac{D_1 - D_2}{D_2} e^{-\frac{1}{2}(D_1 - D_2)^2 k^2 \sigma_v^2} \quad (127)$$

$$= R_{L12} e^{-\frac{1}{2}(D_1 - D_2)^2 \omega^2}, \quad (128)$$

where R_{L12} is the linear response from eq.(30) and we introduced $\omega(k) = k\sigma_v$ as in eq.(77). The computation of R_{11} proceeds along the same lines. A perturbation $\zeta_1(\mathbf{x}_2)$

of the density field at time η_2 does not modify the velocity field and we obtain for $k_1 \neq 0$:

$$\begin{aligned} \psi_1(\mathbf{k}_1, \eta_1) &= \int \frac{d\mathbf{x}_2}{(2\pi)^3} [1 + \delta(\mathbf{x}_2, \eta_2^+)] e^{-i\mathbf{k}_1 \cdot \mathbf{x}_1} \\ &= \int \frac{d\mathbf{x}_2}{(2\pi)^3} e^{-i\mathbf{k}_1 \cdot \mathbf{x}_1} \left[\int d\mathbf{q} \delta_D[\mathbf{x}_2 - \mathbf{q} - D_2 \mathbf{s}_0(\mathbf{q})] + \zeta_1(\mathbf{x}_2) \right] \end{aligned} \quad (129)$$

where we used eq.(97) and $\mathbf{x}_1, \mathbf{x}_2$ are the locations at times η_1, η_2 of the particle of Lagrangian coordinate \mathbf{q} . This gives:

$$R_{11} = \langle \det \left(\frac{\partial \mathbf{x}_2}{\partial \mathbf{q}} \right) e^{-i(D_1 - D_2) \mathbf{k} \cdot \mathbf{s}_0(\mathbf{q})} \rangle. \quad (130)$$

Expanding the determinant we find that most terms cancel out and we obtain the simple result:

$$R_{11} = R_{L11} e^{-\frac{1}{2}(D_1 - D_2)^2 \omega^2}. \quad (131)$$

In a similar fashion, for R_{22} we can write:

$$\begin{aligned} \psi_2(\mathbf{k}_1, \eta_1) &= \int \frac{d\mathbf{q}}{(2\pi)^3} \det \left(\frac{\partial \mathbf{x}_1}{\partial \mathbf{q}} \right) e^{-i\mathbf{k}_1 \cdot \mathbf{x}_1} \int d\mathbf{k} \frac{\mathbf{k}_1 \cdot \mathbf{k}}{k^2} \\ &\times \left[D_1 e^{i\mathbf{k} \cdot \mathbf{q}} \delta_{L0}(\mathbf{k}) + \frac{D_1}{D_2} e^{i\mathbf{k} \cdot \mathbf{x}_2} \zeta_2(\mathbf{k}) \right] \end{aligned} \quad (132)$$

The computation is slightly more intricate than for R_{11} since \mathbf{x}_1 also depends on ζ_2 however most terms cancel out and we recover again the same form as in eqs.(128), (131). Thus, the exact non-linear response function is merely given by:

$$R(k; D_1, D_2) = R_L e^{-\frac{1}{2}(D_1 - D_2)^2 \omega^2}, \quad (133)$$

that is all linear components are multiplied by the same damping factor. We can see from eq.(133) that the response function only depends on the linear power-spectrum through the linear velocity dispersion σ_v^2 , and on scale through $\omega^2 = k^2 \sigma_v^2$. This property extends to the self-energy Σ which is related to R through eq.(71). This is a great simplification with respect to the gravitational dynamics, where the response R and the self-energy Σ depend on the detailed shape of $P_{L0}(k)$, see Valageas (2007). However, even in that case it appears that the behavior of the response function is mostly governed by $\omega^2 = k^2 \sigma_v^2$, see for instance the analysis in sect. 5.2 of Valageas (2007). This also shows that both dynamics share important features.

6.4. Damping self-energy Σ

The self-energy Σ introduced in sect. 4 is usually obtained as a series of diagrams from the path-integral (66). However, since we know the exact response function R we can directly compute Σ from eq.(71). From the simple result (133) we can see that the matrix structure of R , whence of Σ , is not changed by the non-linear corrections. Therefore, from eq.(76) and eq.(133) we write the exact self-energy Σ as:

$$\Sigma(k; D_1, D_2) = \Sigma_0 \sigma[\omega(D_1 - D_2)], \quad (134)$$

where the matrix Σ_0 was obtained in eq.(76), and to generalize the calculation for future use we consider a response of the form:

$$R(k; D_1, D_2) = R_L r(t), \quad t = \omega(D_1 - D_2), \quad r(0) = 1, \quad (135)$$

where the constraint $r(0) = 1$ comes from eq.(29). Substituting eqs.(134)-(135) into eq.(71) yields:

$$r'(t) = - \int_0^t dt' \sigma(t-t') r(t'). \quad (136)$$

The fact that the system (71) can be reduced to eq.(136) shows that the scalings (134)-(135) are indeed self-consistent. We can note that the functions $r(t)$ and $\sigma(t)$ are defined for $t \geq 0$, because of the Heaviside factors $\theta(\eta_1 - \eta_2)$ in R and Σ . Then, introducing the Laplace transform:

$$\tilde{r}(s) = \int_0^\infty dt e^{-st} r(t), \quad (137)$$

we obtain from eq.(136):

$$s\tilde{r}(s) - 1 = -\tilde{\sigma}(s)\tilde{r}(s). \quad (138)$$

For the exact non-linear response (133) we have:

$$r(t) = e^{-t^2/2}, \quad \tilde{r}(s) = \sqrt{\frac{\pi}{2}} e^{s^2/2} \operatorname{erfc}\left(\frac{s}{\sqrt{2}}\right), \quad (139)$$

which gives:

$$\tilde{\sigma}(s) = \sqrt{\frac{2}{\pi}} \frac{e^{-s^2/2}}{\operatorname{erfc}(s/\sqrt{2})} - s, \quad (140)$$

where $\operatorname{erfc}(x)$ is the complementary error function:

$$\operatorname{erfc}(x) = \frac{2}{\sqrt{\pi}} \int_x^\infty dt e^{-t^2}. \quad (141)$$

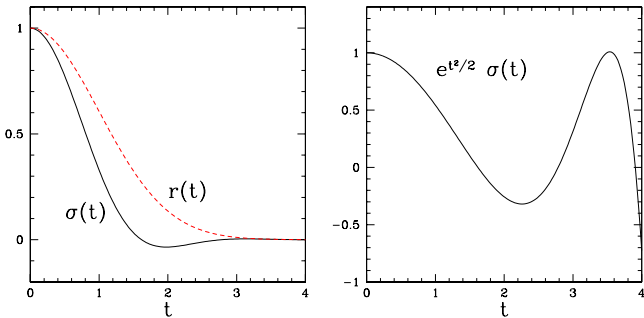


Fig. 2. *Left panel:* the functions $r(t)$ and $\sigma(t)$. *Right panel:* the function $\sigma(t)$ multiplied by a factor $e^{t^2/2}$.

On the other hand, if we write the expansion of $\sigma(t)$ around $t = 0$ as:

$$t \geq 0: \quad \sigma(t) = \sum_{p=0}^{\infty} (-1)^p \sigma_p \frac{t^{2p}}{(2p)!}, \quad (142)$$

we obtain by substituting into eq.(136):

$$\sigma_p = (2p+1)!! - \sum_{m=1}^p \sigma_{p-m} (2m-1)!! \quad (143)$$

and the first few coefficients are:

$$\sigma_0 = 1, \quad \sigma_1 = 2, \quad \sigma_2 = 10, \quad \sigma_3 = 74, \quad \sigma_4 = 706, \dots \quad (144)$$

We can note that this series also appears in other problems of field theory as the number of Feynman diagrams associated for instance to a cubic complex action with two fields (Cvitanovic et al. 1978). This is not surprising since in our case we also have a cubic action (46) with two fields ψ, λ . We show in Fig. 2 the behavior of the self-energy function $\sigma(t)$ computed from the expansion (142). We can see that it shows a fast decay together with oscillations (but the numerical range is too small to check whether the asymptotic is of the form $e^{-t^2/2} \cos(t)$). Thus, the self-energy exhibits a more intricate behavior than the response $r(t)$. This may explain why path-integral methods based on the Schwinger-Dyson equation (71) have difficulties to reproduce the response R from simple approximations to Σ as we shall see below.

6.5. Self-energy II

We can also compute the self-energy Π from eq.(83) which gives:

$$\Pi(x_1, x_2) = (\mathcal{O} - \Sigma).G.(\mathcal{O} - \Sigma)^T \quad (145)$$

where we used eqs.(71)-(72). Then, using the exact expressions of the two-point correlation G and of the self-energy Σ we can obtain Π . However, using the exact two-point correlation G_{ij} would give intricate expressions, as the velocity correlations involve a few prefactors up to order P_{L0}^8 in front of the exponential of eq.(105). Here we are mostly interested in the qualitative behavior of the self-energy Π therefore we shall use the simple approximation:

$$G \simeq \hat{G} \quad \text{with} \quad \hat{G} \equiv G_{11} \begin{pmatrix} 1 & 1 \\ 1 & 1 \end{pmatrix}, \quad (146)$$

where G_{11} is the exact density-density correlation derived in sect. 6.1. The simple form (146) is also consistent with the linear regime limit (27). Then, expanding the exponential of eq.(109) we can write:

$$\hat{G}(k; D_1, D_2) = \int \frac{d\mathbf{q}}{(2\pi)^3} e^{-i\mathbf{k}\cdot\mathbf{q}} \sum_{n=1}^{\infty} \frac{1}{n!} I(\mathbf{q}; \mathbf{k})^n \times \hat{G}_n(k, D_1) \hat{G}_n(k, D_2)^T \quad (147)$$

where $I(\mathbf{q}; \mathbf{k})$ was defined in eq.(107) and we introduced the vectors \hat{G}_n defined by:

$$\hat{G}_n(k, D) = e^{-\omega^2 D^2/2} D^n \begin{pmatrix} 1 \\ 1 \end{pmatrix}. \quad (148)$$

In eq.(147) we used the fact that the term $n = 0$ does not contribute to $\hat{G}(k)$. Then, the self-energy $\hat{\Pi}$ associated with \hat{G} through eq.(145) reads:

$$\hat{\Pi}(k; D_1, D_2) = \int \frac{d\mathbf{q}}{(2\pi)^3} e^{-i\mathbf{k}\cdot\mathbf{q}} \sum_{n=1}^{\infty} \frac{1}{n!} I(\mathbf{q}; \mathbf{k})^n \times \hat{\Pi}_n(k, D_1) \hat{\Pi}_n(k, D_2)^T \quad (149)$$

with:

$$\hat{\Pi}_n(k, D) = (\mathcal{O} - \Sigma) \cdot \hat{G}_n = \hat{\pi}_n(k, D) \begin{pmatrix} 1 \\ 1 \end{pmatrix}. \quad (150)$$

Using eq.(134) we obtain:

$$\hat{\pi}_n(k, D) = (n-1 - \omega^2 D^2) D^n e^{-\omega^2 D^2/2} + \omega^2 D^2 \int_0^D dD' \sigma[\omega(D-D')] D'^{n-1} e^{-\omega^2 D'^2/2}. \quad (151)$$

Then, using eq.(136) we can check that $\hat{\pi}_1 = 0$. Moreover, if we apply the response R to $\hat{\Pi}$ as in eq.(83) we obtain obviously from eq.(150) and eq.(72):

$$R \cdot \hat{\Pi} \cdot R^T = \int \frac{d\mathbf{q}}{(2\pi)^3} e^{-i\mathbf{k}\cdot\mathbf{q}} \sum_{n=2}^{\infty} \frac{1}{n!} I(\mathbf{q}; \mathbf{k})^n \times \hat{G}_n(k, D_1) \hat{G}_n(k, D_2)^T, \quad (152)$$

and we recover the full two-point correlation \hat{G} by noticing that the term $n = 1$ in eq.(147) is equal to $R \times G_I \times R^T$ (with $\eta_I \rightarrow -\infty$) in agreement with eq.(83).

7. Standard perturbative expansions

In this section, we describe the usual perturbative expansion over powers of the linear power-spectrum P_{L0} applied to the Zeldovich dynamics. In this article we shall consider a Λ CDM universe with $\Omega_m = 0.3$, $\Omega_\Lambda = 0.7$, $\Omega_b = 0.046$, $\sigma_8 = 0.9$, a reduced Hubble constant $h = 0.7$ and we shall use the linear power-spectrum given by the CAMB Boltzmann code (Lewis et al. 2000). This gives at $z = 0$ for a smooth linear power-spectrum taken from Eisenstein & Hu (1998):

$$\Delta_{L0}^2(k_0) = 1, \quad \omega(k_0) = 1.3, \quad \text{for } k_0 = 0.21 h \text{Mpc}^{-1}. \quad (153)$$

However, until sect. 13 where we focus on weakly non-linear scales and baryonic acoustic oscillations we shall use a power-law linear power-spectrum (114) with $n = -2$ (except in sect. 10), normalized as in eq.(153):

$$n = -2: \quad \Delta_{L0}^2(k) = k/k_0, \quad (154)$$

where k_0 is given in eq.(153). This has no importance for the response function R , which only depends on $\omega(k) = k\sigma_v$ whatever the linear power-spectrum, but this will allow us to simplify the analysis for the non-linear two-point correlation G . First, we consider the response function R . Expanding eq.(133) over powers of P_{L0} is equivalent to expanding over powers of ω^2 , since $\omega^2 \propto P_{L0}$ from eq.(77).

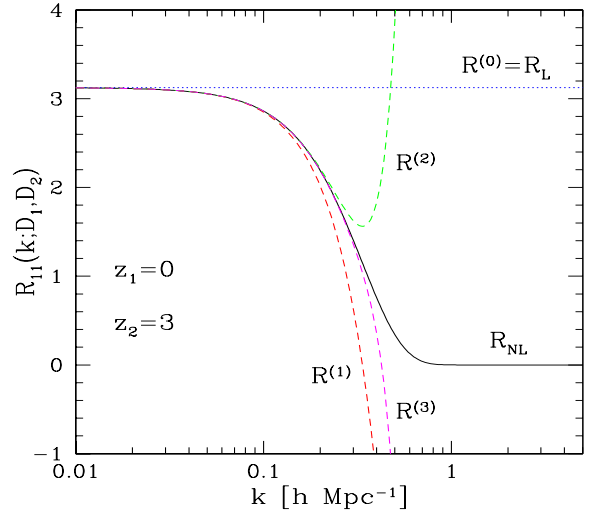


Fig. 3. The standard perturbative expansion of the response function over powers of P_{L0} as in eq.(155). We only show the density-density component R_{11} for clarity. The solid curve R_{NL} is the exact response (133) whereas curves labeled $R^{(p)}$ are the expansion of the response function up to order p over P_{L0} . Here we consider a Λ CDM Universe with “ $n = -2$ ” normalized as in eq.(153) but the results are identical for any CDM cosmology up to a rescaling of k .

Therefore, the response function $R^{(p)}$ expanded up to order P_{L0}^p is:

$$R^{(p)}(k; D_1, D_2) = R_L \sum_{m=0}^p \frac{(-1)^m}{m!} \left[\frac{\omega^2}{2} (D_1 - D_2)^2 \right]^m. \quad (155)$$

This expansion converges absolutely at all times and all scales but the convergence is not uniform. Thus, the convergence rate is very slow for $\omega(D_1 - D_2) \gtrsim 1$ and for any finite order $R^{(p)}$ grows without bound at large times or wavenumbers instead of decreasing. From eq.(155) we can see that in order to obtain a reliable prediction at a given scale we need to go at least up to order $p \sim \omega^2 (D_1 - D_2)^2$. We display the first few terms in Fig. 3, which clearly shows that increasing the order p improves the agreement with the exact result at weakly non-linear scales but worsens the prediction in the highly non-linear regime.

Next, we turn to the standard perturbative expansion of the two-point density-density correlation G_{11} . For illustrative purposes we consider the power-law linear power-spectrum (154). In this case we can perform the integrals in eq.(116) and we obtain for the equal-time non-linear power:

$$\Delta^2 = F(\Delta_{L0}^2) \quad \text{with} \quad F(x) = x \tilde{F}(x\pi/8) \quad (156)$$

and:

$$\tilde{F}(y) = \frac{1}{(1+y^2)^2} + \frac{3y(1+\sqrt{1+y^2}) \text{Arctan} \frac{y}{\sqrt{2+y^2+2\sqrt{1+y^2}}}}{4(1+y^2)^{5/2} \sqrt{2+y^2+2\sqrt{1+y^2}}}$$

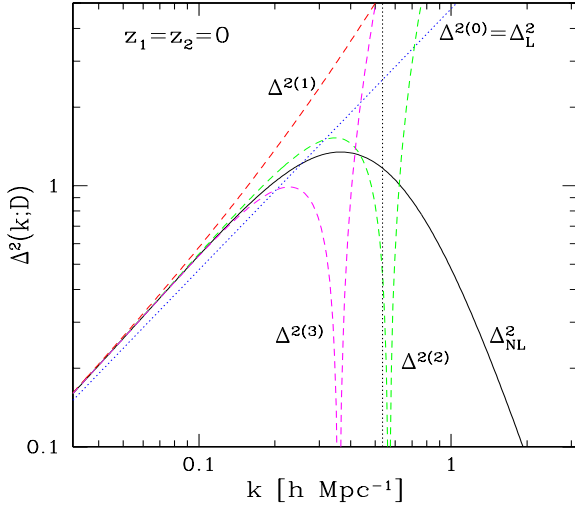


Fig. 4. The standard perturbative expansion of the two-point correlation over powers of P_{L0} from eq.(158). We only show the density-density equal-time logarithmic power $\Delta^2(k; D)$ at redshift $z = 0$, for the case $n = -2$. The solid curve Δ_{NL}^2 is the exact power from eqs.(156)-(157) whereas curves labeled $\Delta^{2(p)}$ are the expansion up to order $p + 1$ over P_{L0} . Higher-order terms grow as k^{p+1} at high wavenumbers. The perturbative expansion diverges beyond the vertical dotted line, for $k > 0.53 h \text{Mpc}^{-1}$.

$$+ \frac{3y(-1 + \sqrt{1+y^2}) \text{Arctan} \frac{y}{\sqrt{2+y^2-2\sqrt{1+y^2}}}}{4(1+y^2)^{5/2} \sqrt{2+y^2-2\sqrt{1+y^2}}}. \quad (157)$$

Note that the last two terms were not correctly written in Taylor & Hamilton (1996). The expansion over powers of P_{L0} corresponds to the expansion of $F(x)$ over powers of x and we obtain:

$$\Delta^2 = \Delta_L^2 + \frac{3\pi^2}{64} \Delta_L^4 - \frac{\pi^2}{32} \Delta_L^6 - \frac{15\pi^4}{8192} \Delta_L^8 + \dots \quad (158)$$

Contrary to the response function, we can see from eq.(157) that this expansion diverges for $\Delta_L^2 > 8/\pi$. Therefore, one cannot describe non-linear scales from this perturbative expansion and going to higher orders only improves the predictions for weakly non-linear scales where $\Delta_L^2 < 8/\pi$. We can see from eqs.(113)-(116) that the radius of convergence of the perturbative series is zero for $n < -2$ (since at large q we encounter an integrand of the form $\int dq e^{-xq^{-n-1}}$ which gives rise to a singularity at $x < 0$). For a Λ CDM cosmology the slope of the linear power-spectrum goes to $n = 1$ at large scales therefore the perturbative series should always converge. However, at small scales where $n \leq -2$ the perturbative expansion is likely to be useless (except for the quasi-linear regime) since the series only converges because of the behavior of the linear power-spectrum at unrelated large scales. We compare the first few terms $\Delta^{2(p)}$ of this perturbative expansion with the exact non-linear power in Fig. 4. In agreement with the analysis above, we can check that the

perturbative predictions provide a good match at quasi-linear scales $\Delta_L^2 \ll 8/\pi, k \ll 0.53 h \text{Mpc}^{-1}$ and becomes useless farther into the non-linear regime.

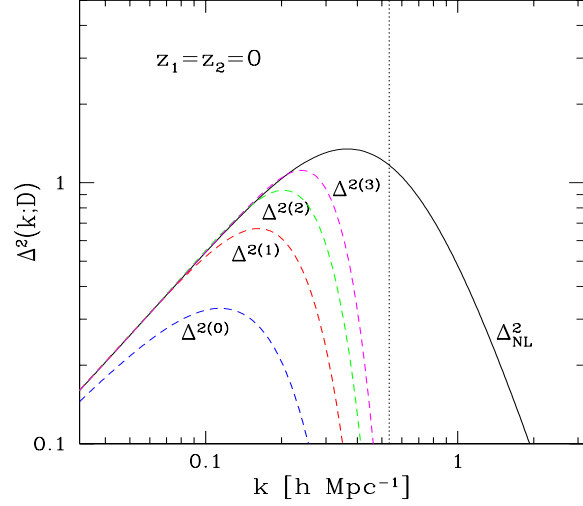


Fig. 5. The perturbative expansion of the two-point correlation over powers of P_{L0} from eq.(159) where we keep apart the exponential factor $e^{-D^2\omega^2}$. The solid curve Δ_{NL}^2 is the exact power from eqs.(156)-(157) whereas curves labeled $\Delta^{2(p)}$ are the expansion up to order $p + 1$ over P_{L0} . All terms decay as $e^{-D^2\sigma_v^2 k^2}$ at high k . The perturbative expansion again diverges beyond the vertical dotted line, for $k > 0.53 h \text{Mpc}^{-1}$.

Crocce & Scoccimarro (2006a) noticed that instead of the standard perturbative expansion (158) one could keep the exponential factor $e^{-(D_1^2+D_2^2)\omega^2/2}$ in expression (109) and only expand the last exponential $e^{D_1 D_2 I}$. In this fashion, all terms of the new series are positive and damped by the exponential factor at small scales, which gives a seemingly better behaved expansion. We display in Fig. 5 the results we obtain for the case $n = -2$ when we consider the series:

$$\begin{aligned} \Delta^2 &= e^{-D^2\omega^2} \left[e^{D^2\omega^2} F(\Delta_L^2) \right] \\ &= e^{-D^2\omega^2} \left[\Delta_L^2 + \left(\frac{3\pi^2}{64} \Delta_L^4 + D^2\omega^2 \Delta_L^2 \right) + \dots \right] \end{aligned} \quad (159)$$

where we used for $\omega(k)$ the normalization of eq.(153). Of course, for a power-law linear power-spectrum we actually have $\omega = \infty$ but eq.(159) describes a CDM-like power-spectrum such that $n = -2$ on the weakly non-linear scales of interest and ω is made finite and normalized to eq.(153) through IR and UV cutoffs. Fig. 159 shows that indeed the terms at each order over P_{L0} are positive and the series looks better behaved. However, it is clear the series still diverges beyond $k \simeq 0.53 h \text{Mpc}^{-1}$ as for (158). Besides, we can note that increasing $\omega(k_0)$ (by moving the IR and UV cutoffs) would move the Gaussian cutoff towards smaller k and would worsen the agreement with the exact non-linear power. In fact, for general power-spectra

where the linear velocity dispersion σ_v^2 is not necessarily governed by the weakly non-linear scales of interest the rewriting associated with eq.(159) does not always improve the agreement with the exact power. Power-law linear power-spectra are a clear example of such cases, since $\omega = \infty$ so that the expansion (159) is not well defined even though the equal-time power remains finite and the usual perturbative expansion (158) is well defined. We can note that the expansion schemes based on eq.(83), through path-integral or diagrammatic methods, do not correspond to the expansion (159). Indeed, although the first term $R \times G_I \times R^T$ may exhibit the factor $e^{-D^2\omega^2}$ this is no longer true for the second term (because of the integrations over time in $R.II.R^T$), as shown by the discussion in sect. 8.3. We can note however that since the response function R also involves the quantity ω we can expect such schemes to fail in cases where the velocity dispersion σ_v^2 is governed by scales which are very far from those of interest.

8. Direct steepest-descent method

8.1. Response R and damping self-energy Σ

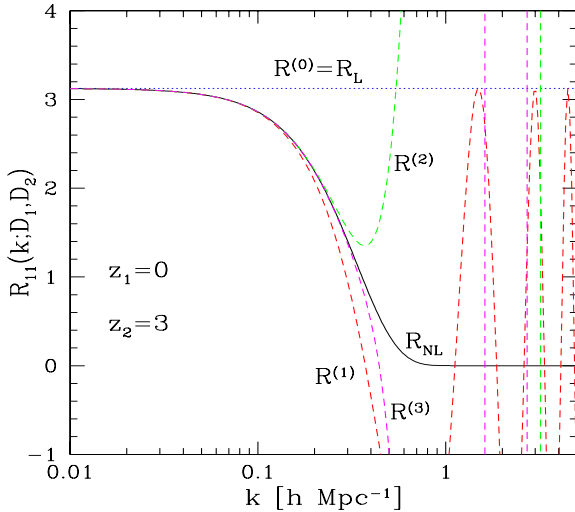


Fig. 6. The expansion of the response function defined by the direct steepest-descent method, from eq.(162). We only show the density-density component R_{11} for clarity. The solid curve R_{NL} is the exact response (133) whereas curves labeled $R^{(p)}$ are the expansion of the response function up to order p .

We now investigate the properties of the steepest-descent method described in sect. 4.1. We first consider the damping self-energy Σ and the response R . The self-energy Σ can be obtained at one-loop order from eq.(73), which gives eq.(76), and at higher orders by including higher-order diagrams. However, for the Zeldovich dynamics it can be directly obtained from the exact expression derived in sect. 6.4. From eq.(134) it is clear that the series (142) corresponds to the perturbative expansion of the

self-energy Σ over powers of P_{L0} (through powers of ω^2). The one-loop result (76) simply corresponds to the first term $\sigma^{(1)}(t) = \sigma_0$ (whereas the linear regime corresponds to $\sigma = 0$) because of the prefactor ω^2 in Σ_0 defined in eq.(76). We obtain in this fashion the self-energy Σ up to order p as:

$$\Sigma^{(p)} = \Sigma_0 \sigma^{(p)} = \Sigma_0 \sum_{m=0}^{p-1} (-1)^m \sigma_m \frac{[\omega(D_1 - D_2)]^{2m}}{(2m)!}. \quad (160)$$

This determines in turns the response function through the steepest-descent method described in sect. 4.1 as:

$$R^{(p)}(k; D_1, D_2) = R_L r^{(p)}[\omega(D_1 - D_2)], \quad (161)$$

where $r^{(p)}(t)$ is obtained from $\sigma^{(p)}(t)$ through eq.(136). From eq.(138) this gives:

$$\tilde{r}^{(p)}(s) = \frac{s^{2p-1}}{s^{2p} + \sum_{m=0}^{p-1} (-1)^m \sigma_m s^{2(p-1-m)}}. \quad (162)$$

This gives for the first few terms:

$$r^{(0)} = 1, \quad r^{(1)} = \cos t, \quad r^{(2)} = \frac{1}{3} \cosh t + \frac{2}{3} \cos \sqrt{2}t. \quad (163)$$

Indeed, the perturbative expansion of the self-energy Σ gives $\sigma(t)$ as a series over powers of t whence $\tilde{\sigma}(s)$ as a series over powers of $1/s$. This yields a rational function for $\tilde{r}^{(p)}(s)$ and a sum of exponentials for $r^{(p)}(t)$. At order $p = 1$ the arguments of the exponentials are imaginary (they are given by the roots of the denominator of $\tilde{r}^{(p)}(s)$) but it appears that at order $p = 2, 3$ (and presumably at higher orders) real parts appear. Since the denominator is even, see eq.(162), the roots appear by pairs $\pm s_i$ so that both decaying and growing exponentials appear. Therefore, the direct steepest-descent method cannot reproduce the decay of the response function at large t (i.e. in the highly non-linear regime). Of course, at a given order p the response $r^{(p)}(t)$ agrees with the expansion of the exact response (155) up to order t^{2p} . We display in Fig. 6 the first few terms $R^{(p)}$. The behavior is actually rather close to the standard perturbative expansion shown in Fig. 3 as the higher orders slowly improve the agreements over weakly non-linear scales but explode increasingly fast into the highly non-linear regime (but their amplitude grows even faster as exponentials instead of power-laws).

8.2. Padé approximants

The remarks above suggest that we may improve the expansion (162) by looking for a Padé approximant to the rational function $\tilde{r}^{(p)}(s)$ which has the same expansion over $1/s$ up to $1/s^{2p+1}$. In fact, since we know the exact response function we can directly obtain the series of Padé approximants from eq.(139). First, from the expansion of $e^{-t^2/2}$ at $t = 0$ we obtain formally the expansion of $\tilde{r}(s)$ over $1/s$ as:

$$\tilde{r}(s) = \sum_{p=0}^{\infty} (-1)^p (2p-1)!! s^{-2p-1}. \quad (164)$$

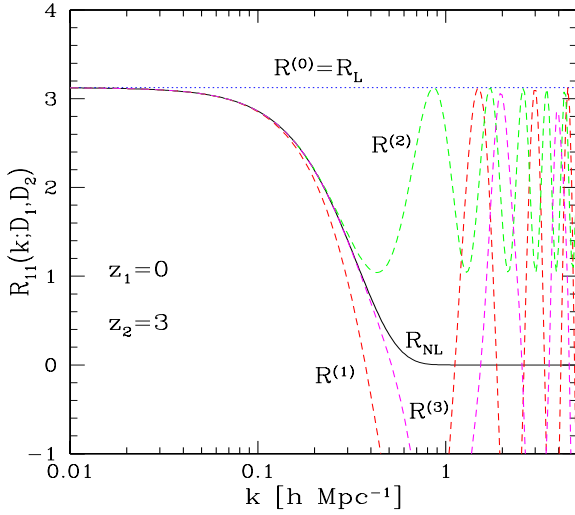


Fig. 7. The expansion of the response function defined by the Padé approximants from eqs.(171). At each order one obtains a sum of cosines, with an offset for even p .

Note that this only provides an asymptotic series for $\tilde{r}(s)$ in the limit $s \rightarrow \infty$. Here it is convenient to make the change of variable $y = 2/s^2$ and to define $\bar{r}(y)$ by:

$$\tilde{r}(s) = \frac{1}{s} \bar{r}(y = 2/s^2), \quad \bar{r}(y) = \sum_{p=0}^{\infty} (-1)^p \bar{r}_p y^p. \quad (165)$$

From eq.(164) we obtain for the coefficients \bar{r}_p :

$$\bar{r}_p = \frac{(2p-1)!!}{2^p} = \frac{\Gamma[p+1/2]}{\sqrt{\pi}} = \int_0^{\infty} \frac{dt}{\sqrt{\pi t}} e^{-t} t^p. \quad (166)$$

This shows that the expansion (165) is a Stieltjes series since the coefficients \bar{r}_p are the moments of a real positive function defined over $t \geq 0$ (here of the function $e^{-t}/\sqrt{\pi t}$), see Bender & Orszag (1978). Since Carleman's condition is fulfilled, $\sum \bar{r}_p^{-1/2p} = \infty$, the function $\bar{r}(y)$ is uniquely determined by its asymptotic expansion (165) which can be resummed as:

$$\bar{r}(y) = \int_0^{\infty} \frac{dt}{1+yt} \frac{e^{-t}}{\sqrt{\pi t}}. \quad (167)$$

Then, all coefficients of the continued-fraction representation of $\bar{r}(y)$ are nonnegative and both Padé sequences P_p^p and P_{p+1}^p converge monotonically to $\bar{r}(y)$ as:

$$P_1^0(y) \leq P_2^1(y) \leq P_3^2(y) \leq \dots \leq \bar{r}(y) \quad (168)$$

$$\bar{r}(y) \leq \dots \leq P_2^2(y) \leq P_1^1(y) \leq P_0^0(y) \quad (169)$$

and:

$$\bar{r}(y) = \lim_{p \rightarrow \infty} P_{p+1}^p(y) = \lim_{p \rightarrow \infty} P_p^p(y). \quad (170)$$

By contrast, the usual perturbative expansion (155), which is associated with the expansion (164), amounts to approximate $\bar{r}(y)$ by a polynomial, that is by the sequence $P_p^0(y)$, whereas the steepest-descent method (162)

amounts to approximate $1/\bar{r}(y)$ by a polynomial, that is $\bar{r}(y)$ by the sequence $P_p^0(y)$. As we have seen above these two sequences do not converge very well since they give a response $r^{(p)}(t)$ which grows without bound for $t \rightarrow \infty$. On the other hand, the sequence associated with (170) gives:

$$\begin{aligned} \bar{r}^{(0)}(y) &= P_0^0 = 1, \quad \bar{r}^{(1)}(y) = P_1^0 = \frac{1}{1+y/2}, \\ \bar{r}^{(2)}(y) &= P_1^1 = \frac{1+y}{1+3y/2}, \dots \end{aligned} \quad (171)$$

The first two terms give the same results $r^{(0)}$ and $r^{(1)}$ as eq.(163) but the next two terms give:

$$\begin{aligned} r^{(2)}(t) &= \frac{2}{3} + \frac{1}{3} \cos \sqrt{3}t, \\ r^{(3)}(t) &= \frac{\sqrt{6}+2}{2\sqrt{6}} \cos \sqrt{3-\sqrt{6}}t \\ &\quad + \frac{\sqrt{6}-2}{2\sqrt{6}} \cos \sqrt{3+\sqrt{6}}t, \end{aligned} \quad (173)$$

which do not grow exponentially at large t any more. Indeed, because both the sequences P_p^p and P_{p+1}^p and $\bar{r}(y)$ are Stieltjes functions they are analytic in the cut plane $|\arg(y)| < \pi$ and all poles of the Padé approximants P_p^p and P_{p+1}^p lie on the negative real axis (Bender & Orszag 1978). Therefore, eq.(165) shows that all poles of the associated rational function $\tilde{r}^{(p)}(s)$ lie on the imaginary axis and appear by pairs $\pm is_j$ together with a pole at $s = 0$ for even p . Then, the response factor $r^{(p)}(t)$ is a sum of cosines $\cos(s_j t)$ plus a constant for even p , in agreement with eqs.(172)-(173). This is a clear improvement over the standard expansion (155) and the direct steepest-descent expansion (162)-(163). However, even this expansion cannot recover the Gaussian decay $e^{-t^2/2}$ which is replaced by fast oscillations. Nevertheless, this gives rise to an effective damping (for odd p) once the response function is integrated with some weight function. We compare the first few terms to the exact non-linear response in Fig. 7. Of course, we recover the same agreement at low k as with the other expansions displayed in Fig. 3 and Fig. 6, but as explained above the response remains bounded at high k with fast oscillations.

8.3. Correlation G and self-energy II

We now consider the predictions of the direct steepest-descent method for the two-point correlation G and self-energy II. As in sect. 7 we shall consider the case of a power-law linear power-spectrum $n = -2$ which simplifies the calculations since integrals over wavenumber k are already performed following eqs.(156)-(157). Moreover, as for eq.(159) and Fig. 5 we consider a finite linear velocity dispersion $\omega(k) = k\sigma_v$ normalized as in eq.(153). As in sect. 6.5, in order to simplify the computations we approximate the matrix form of the correlation G_{ij} by eq.(146). Thus, we keep the exact non-linear density-density correlation G_{11} and we make approximation $G_{ij} = G_{11}$ for

all $\{i, j\}$. Using eq.(112) and expanding the exponential $e^{D_1 D_2 \omega^2}$ and $F(x)$ we write G_{11} as:

$$G_{11} = \frac{1}{4\pi k^3} \sum_{p,m=0}^{\infty} \frac{F_p}{p!m!} \Delta_{L0}^{2p} \omega^{2m} (D_1 D_2)^{p+m} e^{-\frac{D_1^2 + D_2^2}{2} \omega^2} \quad (174)$$

where F_p is the p -th derivative of $F(x)$ at $x = 0$:

$$F(x) = \sum_{p=0}^{\infty} \frac{F_p}{p!} x^p. \quad (175)$$

The first few coefficients F_p are given in eq.(158). Note however that for the case $n = -2$ the Taylor series (175) diverges for $x > 8/\pi$ as seen in sect. 7. Then, we can write the matrix two-point correlation \hat{G} as:

$$\hat{G} = \frac{1}{4\pi k^3} \sum_{p,m} \frac{F_p}{p!m!} \Delta_{L0}^{2p} \omega^{2m} \hat{G}_{p+m}(D_1) \hat{G}_{p+m}(D_2)^T, \quad (176)$$

where the vectors \hat{G}_n were defined in eq.(148). Thus, as compared with eq.(147) the use of a power-law linear power-spectrum has simply replaced the integral over \mathbf{q} by a discrete sum. Then eqs.(149)-(152) still apply once we replace the integral over \mathbf{q} by this discrete sum. Thus, we now need to compute the functions $\hat{\pi}_n(D)$ defined in eq.(151). Using the expansion (142) we can perform the integrations over D' and we obtain:

$$\begin{aligned} \hat{\pi}_n(D) &= (n-1)D^n + D^n \sum_{m=0}^{\infty} \frac{(-1)^m}{m!} \left(\frac{\omega^2 D^2}{2} \right)^{m+1} \\ &\times \left[-\frac{n-1}{m+1} - 2 + \frac{m! 2^{m+1}}{(n+2m)!} \sum_{\ell=0}^m \sigma_{m-\ell} \frac{(n+2\ell-1)!}{\ell! 2^\ell} \right] \quad (177) \end{aligned}$$

Of course, from eq.(143) we can check that $\hat{\pi}_1 = 0$ in agreement with the result already obtained in sect. 6.5. Substituting eq.(177) into the analog of eq.(149), which reads here (as eq.(176) for \hat{G}):

$$\hat{\Pi} = \frac{1}{4\pi k^3} \sum_{p,m} \frac{F_p}{p!m!} \Delta_{L0}^{2p} \omega^{2m} \hat{\Pi}_{p+m}(D_1) \hat{\Pi}_{p+m}(D_2)^T, \quad (178)$$

we obtain the self-energy $\hat{\Pi}$ up to order P_{L0}^{p+1} as:

$$\hat{\Pi}^{(p)}(k; D_1, D_2) = \frac{1}{4\pi k^3} \sum_{n=1}^p \hat{\Pi}_n(k; D_1, D_2) \begin{pmatrix} 1 & 1 \\ 1 & 1 \end{pmatrix} \quad (179)$$

where $\hat{\Pi}_n \propto P_{L0}^{n+1}$ and the first few terms are:

$$\hat{\Pi}_1 = \Delta_L^2 \left(\frac{3\pi^2}{64} \Delta_L^2 + \omega_1 \omega_2 \right) \quad (180)$$

$$\begin{aligned} \hat{\Pi}_2 &= -\Delta_L^2 (\omega_1^2 + \omega_2^2) \left(\frac{3\pi^2}{64} \Delta_L^2 + \omega_1 \omega_2 \right) \\ &+ \Delta_L^2 \left(-\frac{\pi^2}{8} \Delta_L^4 + \frac{3\pi^2}{16} \Delta_L^2 \omega_1 \omega_2 + 2\omega_1^2 \omega_2^2 \right) \quad (181) \end{aligned}$$

where we introduced (we recall that $\Delta_L^2 = D_1 D_2 \Delta_{L0}^2$):

$$\omega_1 = D_1 \omega(k) = D_1 k \sigma_v, \quad \omega_2 = D_2 \omega(k). \quad (182)$$

As for the standard perturbative expansion (158) applied to the correlation function G , the series expansion (179) for the self-energy $\hat{\Pi}$ gives higher-order terms which grow increasingly fast into the highly non-linear regime. Moreover, we can expect that it diverges at equal times for $\Delta_L^2 > 8/\pi$ as for G .

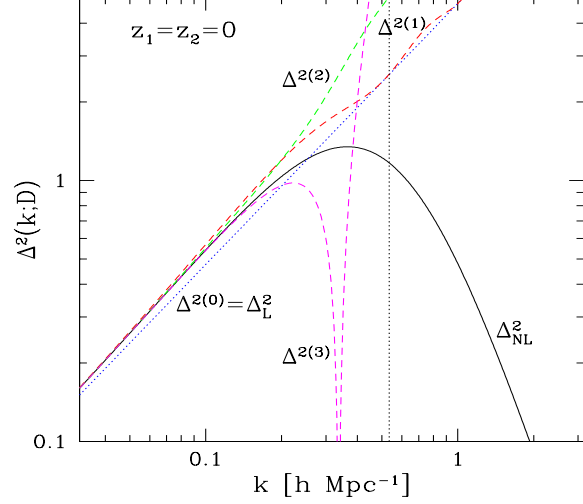


Fig. 8. The expansion of the two-point correlation defined by the direct steepest-descent method, from eq.(179). Higher-order terms display an exponential growth at high k for $p \geq 2$.

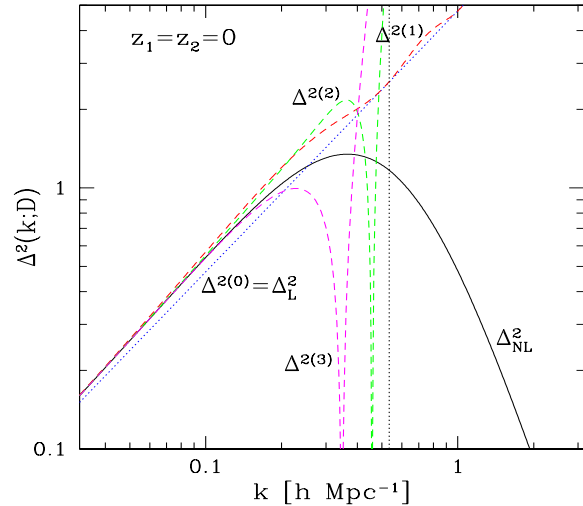


Fig. 9. The expansion of the two-point correlation defined by the direct steepest-descent method, from eq.(179), but using the Padé approximants (172)-(173) for the response function. Higher-order terms display a power-law growth at high k .

Then, the direct-steepest descent method prediction at order p is obtained by applying eq.(83) using the response $R^{(p)}$ and the self-energy $\hat{\Pi}^{(p)}$ at that order. Note that this expansion has not the form of a standard perturbative

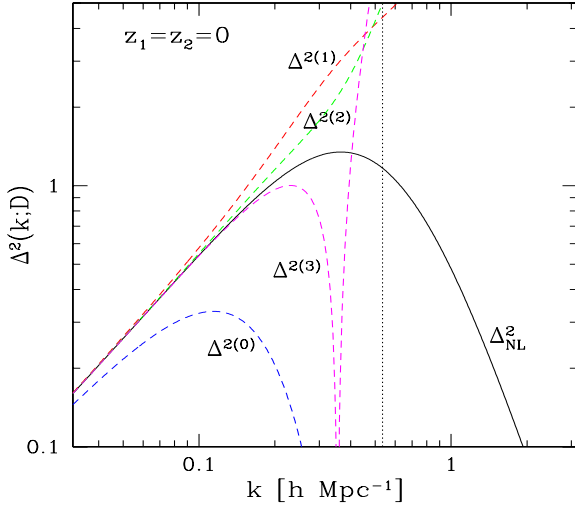


Fig. 10. The expansion of the two-point correlation defined by the direct steepest-descent method, from eq.(179), but using the exact response function (133). Higher-order terms display a power-law growth at high k .

expansion such as eq.(158) or eq.(159) since as we go to higher orders all terms in the series get modified as compared with the result at a lower order since the response $R^{(p)}$ has a different functional form, see (163). At linear order $p = 0$ we have $\Pi = 0$ and $\Delta^2 = \Delta_L^2$. At first order $p = 1$ we obtain from eq.(163):

$$\Delta^{2(1)}(k; D_1, D_2) = \Delta_L^2 \cos(\omega_1) \cos(\omega_2) + \Delta_L^2 \left(\frac{3\pi^2}{64} \Delta_L^2 + \omega_1 \omega_2 \right) \frac{\sin(\omega_1) \sin(\omega_2)}{\omega_1 \omega_2}. \quad (183)$$

Of course, if we expand eq.(183) over powers of ω we recover the usual perturbative result and at equal time we recover eq.(158) up to order Δ_L^4 . Moreover, we already know that at equal times $D_1 = D_2$ all terms ω must cancel out up to order P_{L0}^{p+1} because the exact power (156) does not depend on ω . This is a general result which does not depend on the shape of the linear power-spectrum and can be seen from eq.(105). This is related to the cancellation of IR divergences recalled in sect. 6.2 associated with Galilean invariance. In a similar fashion, at order $p = 2$ we obtain from eq.(163):

$$\begin{aligned} \Delta^{2(2)} &= \Delta_L^2 r_1^{(2)} r_2^{(2)} + \Delta_L^2 \left(\frac{3\pi^2}{64} \Delta_L^2 + \omega_1 \omega_2 \right) r_1^{(2;1)} r_2^{(2;1)} \\ &\quad - \Delta_L^2 \left(\frac{3\pi^2}{64} \Delta_L^2 + \omega_1 \omega_2 \right) \left(\omega_1^2 r_1^{(2;3)} r_2^{(2;1)} + \omega_2^2 r_1^{(2;1)} r_2^{(2;3)} \right) \\ &\quad + \Delta_L^2 \left(-\frac{\pi^2}{8} \Delta_L^4 + \frac{3\pi^2}{16} \Delta_L^2 \omega_1 \omega_2 + 2\omega_1^2 \omega_2^2 \right) r_1^{(2;2)} r_2^{(2;2)} \end{aligned} \quad (184)$$

where we defined ($\ell \geq 1$):

$$r_i^{(p)} = r^{(p)}(\omega_i), \quad r_i^{(p;\ell)} = \int_0^1 dt t^{\ell-1} r^{(p)}[\omega_i(1-t)]. \quad (185)$$

We display in Fig. 8 our results for the first few terms. We can see that the exponential terms associated with the re-

sponse function (see eq.(163)) make the higher-order approximations grow exponentially at high k (for $p \geq 2$). This very strong growth makes the series of little practical value for $p \geq 2$ where the convergence is not better than for the standard perturbative expansion displayed in Fig. 4. We can note that the equal-time power can become negative at high k whereas both Π and G should be positive matrices from eq.(83), which implies that the components G_{ii} and Π_{ii} are positive at equal times. This failure comes from the truncation of the self-energy $\hat{\Pi}$ in eq.(179) which breaks the positivity of $\hat{\Pi}$. Indeed, from eq.(181) and the scalings $\Delta_L^2 \propto k$ and $\omega \propto k$ we see that $\hat{\Pi}_2 \sim -3\pi^2/32 \Delta_L^4 \omega^2$ at high k .

We show in Fig. 9 the results obtained from the expansion (179) for the self-energy $\hat{\Pi}$ but using the Padé approximants (172)-(173) for the response function. The higher-order terms no longer grow as exponentials at high k but as power-laws, since the response functions only contain constants and cosines instead of exponentials. However, this is not sufficient to significantly improve the convergence of the series to the exact non-linear power Δ^2 .

Finally, we show in Fig. 10 the results obtained from the expansion (179) for the self-energy $\hat{\Pi}$ when we use the exact response function (133). Note that in this case the lowest-order approximation $\Delta^{2(0)}$ is equal to the linear power multiplied by a Gaussian damping factor. It is actually equal to the first term of eq.(159). Higher-order terms do not exhibit such a Gaussian damping because of the time-integrals involved in the last term of eq.(83). Indeed, the expansion (179) yields power-laws over D_1, D_2 and this gives enough power generated at all times to build large density fluctuations into the non-linear regime. We can see from Fig. 10 that using the exact response function is not sufficient to significantly improve the convergence of the series obtained for the matter power-spectrum. Therefore, it appears that in order to improve the results one should use other expansion schemes for the self-energy $\hat{\Pi}$: improving the response function alone does not help much.

8.4. Using a Gaussian decay for the self-energy Π

The previous discussion and the results obtained from the expansion (159), shown in Fig. 5, suggest that it may be useful to factor out a Gaussian term of the form $e^{-D^2 \omega^2}$ from the self-energy Π . Therefore, we now replace the expansion (179) by:

$$\hat{\Pi}(k; D_1, D_2) = \frac{e^{-(\omega_1^2 + \omega_2^2)/2}}{4\pi k^3} \sum_{n=1}^{\infty} \hat{\Pi}_n(k; D_1, D_2) \begin{pmatrix} 1 & 1 \\ 1 & 1 \end{pmatrix} \quad (186)$$

where $\hat{\Pi}_n$ is again of order P_{L0}^{n+1} and $\omega_i = D_i \omega$ as in eq.(182). This expansion can be obtained as in sect. 8.3 or it can be derived from the expansion (179) by multiplying by a factor $e^{-(\omega_1^2 + \omega_2^2)/2}$ and expanding again over powers of P_{L0} . We display in Fig. 11 the results obtained from eq.(186) using the exact response function (133) which also shows a Gaussian decay at high k . Of course, because

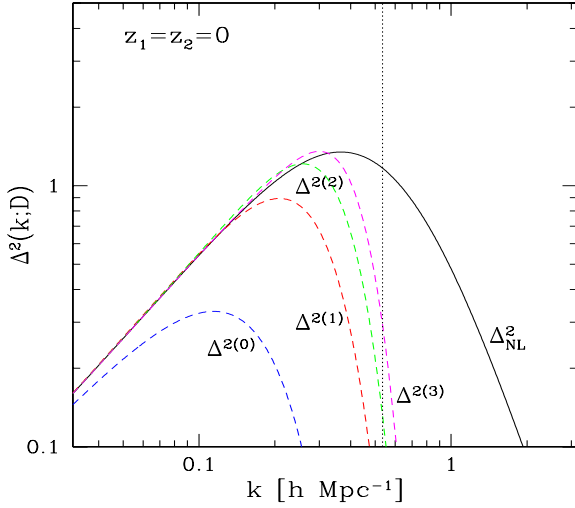


Fig. 11. The expansion of the two-point correlation from eq.(186), using the exact response function (133) and the expansion (186) with Gaussian factors for the self-energy $\hat{\Pi}$. All terms display a Gaussian decay at high k .

of the Gaussian damping factor introduced in eq.(186) all terms decay as $e^{-k^2\sigma_v^2}$ at high k and the expansion looks better behaved than the one displayed in Fig. 10. Besides, the approximation obtained at a given order seems to provide a good accuracy over a slightly larger range than in both Fig. 10 and Fig. 5. Thus, decomposing the two-point correlation in terms of response function and self-energy as in eq.(83) and using a Gaussian decay ansatz at high k appears to be a good scheme. However, this is somewhat artificial (see sect. 9).

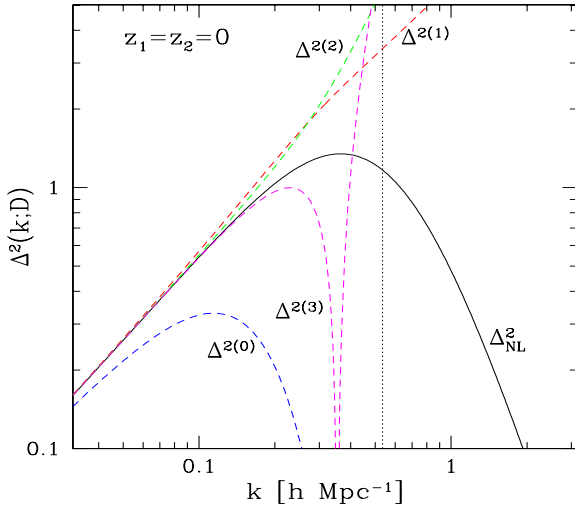


Fig. 12. The expansion of the two-point correlation from eq.(187), using the exact response function (133) and the expansion (187) with Gaussian factors for the self-energy $\hat{\Pi}$. This Gaussian factor only damps the contributions at different times and high-order terms display a power-law growth at high k .

As explained in sect. 9 below, the Gaussian damping factors $e^{-D^2k^2\sigma_v^2/2}$ merely correspond to the linear displacement field which moves the location of large-scale structures between different times. However, this process does not affect the matter clustering and in particular the linear velocity variance σ_v can show IR divergences for $n \leq -1$ which cancel out for equal-time statistics (Vishniac 1983; Jain & Bertschinger 1996). This suggests that it would make more sense to factor out a Gaussian factor of the form:

$$\hat{\Pi}(k; D_1, D_2) = \frac{e^{-(\omega_1 - \omega_2)^2/2}}{4\pi k^3} \sum_{n=1}^{\infty} \hat{\Pi}_n(k; D_1, D_2) \begin{pmatrix} 1 & 1 \\ 1 & 1 \end{pmatrix} \quad (187)$$

which is equal to unity at equal times. This also agrees with the functional form of the exact two-point function (112) and of the simple approximation (199) below. We show in Fig. 12 the results of the expansion (187), using again the exact response function (133). The high-order terms now grow as power-laws at high k for the equal-time power (clearly they would still decay as a Gaussian for unequal times) but the expansion does not fare better than the straightforward expansion obtained from eq.(179) displayed in Fig. 10. This shows that using a reasonable Gaussian decay ansatz (which must disappear at equal times) is not sufficient to bring a significant improvement over previous expansions.

9. High- k limit ?

In order to improve the behavior of expansion schemes Crocce & Scoccimarro (2006b) suggested to use a response function which matches both the low- t behavior (obtained by perturbative expansions) and the Gaussian decay at high t . Indeed, for the case of the gravitational dynamics, where the exact response R is not known, one can still obtain the low- t behavior by perturbative expansions such as those described above by summing over higher-loop diagrams, see Crocce & Scoccimarro (2006a) and Valageas (2007). On the other hand, Crocce & Scoccimarro (2006b) managed to resum a subset of diagrams in the high- k limit which gives rise to the same Gaussian decay $e^{-t^2/2}$ as for the Zeldovich dynamics. Then, one may hope that by using a “fit” for the response function which closely follows the expected behavior one has made half the work needed to obtain a good prescription for the matter power-spectrum and it only remains to use a good recipe for the self-energy Π . In fact, we have shown in sect. 8.3 and Fig. 10 that this is not so simple because even using the exact response R is not enough to improve the predictions for the power-spectrum if we use a simple expansion over powers of P_{L0} for the self-energy Π , as in eq.(179). Besides, as shown in sect. 8.4 using such a Gaussian cutoff for Π is not sufficient either.

Nevertheless, we revisit in this section the approximate resummation performed in Crocce & Scoccimarro (2006b) to clarify its meaning and its shortcomings. Let us start from the general integral equation of motion (51). This

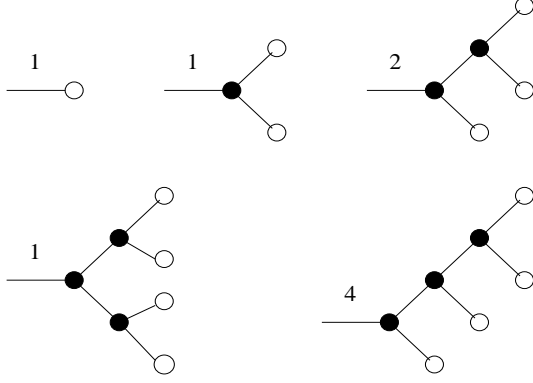


Fig. 13. The expansion of the non-linear field ψ over the linear growing mode ψ_L from eq.(51), up to order ψ_L^4 . The filled circles are the vertex \tilde{K}_s whereas the white circles are the linear input ψ_L . The numbers are the multiplicity factor associated with each diagram.

equation can be solved perturbatively as an expansion over powers of ψ_L of the form:

$$\psi = \psi_L + \tilde{K}_s \psi_L^2 + 2\tilde{K}_s^2 \psi_L^3 + 5\tilde{K}_s^3 \psi_L^4 + \dots \quad (188)$$

which can also be written in a diagrammatic manner, see Crocce & Scoccimarro (2006a), Valageas (2001), as shown in Fig. 13. Next, in the high- k limit one assumes that all wavenumbers w_i associated with the linear fields ψ_L are much smaller than k except for one field (because of the conservation of momentum associated with the Dirac factor $\delta_D(\mathbf{k}_1 + \mathbf{k}_2 - \mathbf{k})$ in the vertex K_s , see eq.(20)). This assumes that the power is generated over some finite range of wavenumbers (i.e. the dynamics is not governed by an extended UV tail). Besides, Crocce & Scoccimarro (2006b) assumed that the dominant contribution is provided by the diagrams shown in Fig.14 where all low- w_i fields $\psi_L(\mathbf{w}_i)$ are directly connected to the “principal path” which joins the only one high- k field ψ_L to the root of the diagram. The idea is that in such diagrams the “principal path” only interacts with other fields $\psi_L(\mathbf{w}_i)$ which are pure linear growing modes, as they have not already suffered non-linear interactions through the coupling vertex \tilde{K}_s . Then, these diagrams should maximize the cross-correlations since non-linear interactions are expected to erase the memory of initial conditions. Therefore, the response function R may be dominated by these diagrams in the high- k limit.

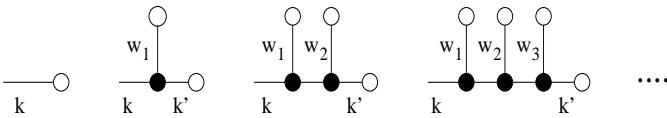


Fig. 14. The diagrams which are assumed to dominate in the high- k limit. We have $k' \simeq k$ and all intermediate wavenumbers w_i are much smaller than k .

On the other hand, we note that the diagrams of Fig.14 are actually generated by the equation of motion:

$$\hat{\psi}(x) = \psi_L(x) + 2\tilde{K}_s(x; x_1, x_2) \cdot \psi_L^<(x_1) \hat{\psi}(x_2) \quad (189)$$

where $\psi_L^<(x_1)$ is the linear growing mode restricted to low wavenumbers $w_1 \ll k$ (the factor 2 comes from the fact that we can associate $\psi_L^<$ to either x_1 or x_2 in eq.(51)) and we noted by a hat the approximate field $\hat{\psi}$ obtained in this high- k limit. Note that $\psi_L(x)$ and $\psi_L^<(x_1)$ are *independent* Gaussian fields (since $w_1 \neq k$) and eq.(189) is now a *linear* equation for the field $\hat{\psi}$. Indeed, we can check that by solving eq.(189) as a perturbative series over powers of ψ_L we recover the diagrams of Fig.14. In other words, by keeping only the diagrams of Fig.14 we have actually approximated the non-linear equation of motion (51) by the linear equation of motion (189). Next, following Crocce & Scoccimarro (2006b) we note that the vertices γ^s of eqs.(21)-(22) satisfy in the high- k limit:

$$\frac{k}{w} \gg 1: \sum_m \gamma_{i;m_j}^s(\mathbf{w}, \mathbf{k}) \psi_{Lm}^<(\mathbf{w}, \eta') \simeq \delta_{i,j} \frac{\mathbf{k} \cdot \mathbf{w}}{2w^2} e^{\eta'} \delta_{L0}(\mathbf{w}) \quad (190)$$

where we only kept the terms of order k/w and we neglected terms of order 1, $w/k, \dots$. At this level we can also replace the Dirac factor $\delta_D(\mathbf{w} + \mathbf{k}' - \mathbf{k})$ by $\delta_D(\mathbf{k}' - \mathbf{k})$ in the vertex K_s and using the second eq.(52) and eq.(20) we can write eq.(189) as:

$$\hat{\delta}(\mathbf{k}, \eta) = e^{\eta} \delta_{L0}(\mathbf{k}) + \int d\mathbf{w} \frac{\mathbf{k} \cdot \mathbf{w}}{w^2} \delta_{L0}(\mathbf{w}) e^{\eta} \int_{\eta_I}^{\eta} d\eta' \hat{\delta}(\mathbf{k}, \eta') \quad (191)$$

where we used the fact that ψ_L is also the linear growing mode. Here we considered the case where the initial conditions are set up at a finite time η_I as in sect. 3.2.2. This linear equation can be solved through the expansion:

$$\hat{\delta}(\mathbf{k}, \eta) = e^{\eta} \delta_{L0}(\mathbf{k}) + e^{\eta} \delta_{L0}(\mathbf{k}) \sum_{p=1}^{\infty} \prod_{j=1}^p \int d\mathbf{w}_j \frac{\mathbf{k} \cdot \mathbf{w}_j}{w_j^2} \delta_{L0}(\mathbf{w}_j) \times \int_{\eta_I}^{\eta} d\eta_1 e^{\eta_1} \int_{\eta_I}^{\eta_1} d\eta_2 e^{\eta_2} \dots \int_{\eta_I}^{\eta_{p-1}} d\eta_p e^{\eta_p} \quad (192)$$

which can be resummed as:

$$\hat{\delta}(\mathbf{k}, D) = D \delta_{L0}(\mathbf{k}) e^{(D-D_I)} \int d\mathbf{w} \frac{\mathbf{k} \cdot \mathbf{w}}{w^2} \delta_{L0}(\mathbf{w}), \quad (193)$$

where we used the time-coordinate $D = e^{\eta}$. Let us recall that $\delta_{L0}(\mathbf{k})$ and $\delta_{L0}(\mathbf{w})$ must be treated as independent Gaussian variables in eq.(193). Then, if we define a response $\hat{R}_I(\mathbf{k}, \eta; \mathbf{k}')$ in a fashion similar to eq.(63) by:

$$\hat{R}_I(\mathbf{k}, \eta; \mathbf{k}') = \left\langle \frac{\mathcal{D} \hat{\delta}(\mathbf{k}, \eta)}{\mathcal{D} \hat{\delta}_{LI}(\mathbf{k}')} \right\rangle = \frac{1}{D_I} \left\langle \frac{\mathcal{D} \delta(\mathbf{k}, \eta)}{\mathcal{D} \delta_{L0}(\mathbf{k}')} \right\rangle, \quad (194)$$

where \mathcal{D} is the functional derivative, we obtain:

$$\hat{R}_I = \delta_D(\mathbf{k} - \mathbf{k}') \frac{D}{D_I} \left\langle e^{(D-D_I)} \int d\mathbf{w} \frac{\mathbf{k} \cdot \mathbf{w}}{w^2} \delta_{L0}(\mathbf{w}) \right\rangle = \delta_D(\mathbf{k} - \mathbf{k}') \frac{D}{D_I} e^{-\frac{1}{2}(D-D_I)^2 k^2 \sigma_w^2}. \quad (195)$$

Thus we recover the exact Gaussian decay at high k obtained by Crocce & Scoccimarro (2006b). Note that since we restricted the initial conditions to the linear growing mode in eq.(191) the response \hat{R}_I of eq.(194) actually corresponds to the sum $\hat{\mathcal{R}}_{11} + \hat{\mathcal{R}}_{12}$ of the components of the response defined in eq.(63). The advantage of this formulation is that one may see more clearly through eqs.(189)-(193) the meaning of the assumptions involved in this high- k limit. In particular, it is interesting to compare eq.(193) with the exact result (98) which reads:

$$\delta(\mathbf{k}, D) = \int \frac{d\mathbf{q}}{(2\pi)^3} e^{-i\mathbf{k}\cdot\mathbf{q}} e^D \int d\mathbf{w} e^{i\mathbf{w}\cdot\mathbf{q}} \frac{\mathbf{k}\cdot\mathbf{w}}{w^2} \delta_{L0}(\mathbf{w}). \quad (196)$$

Then, if we assume that we can split the integral over \mathbf{w} into low and high wavenumber parts $w < \Lambda$ and $w > \Lambda$, such that most of the power is associated with $w < \Lambda$ and the high-wavenumber contribution is small, we can expand the exponential over this high-wavenumber part as:

$$\begin{aligned} \delta(\mathbf{k}, D) &\simeq \int \frac{d\mathbf{q}}{(2\pi)^3} e^{-i\mathbf{k}\cdot\mathbf{q}} e^D \int_{w<\Lambda} d\mathbf{w} e^{i\mathbf{w}\cdot\mathbf{q}} \frac{\mathbf{k}\cdot\mathbf{w}}{w^2} \delta_{L0}(\mathbf{w}) \\ &\quad \times D \int_{w'>\Lambda} d\mathbf{w}' e^{i\mathbf{w}'\cdot\mathbf{q}} \frac{\mathbf{k}\cdot\mathbf{w}'}{w'^2} \delta_{L0}(\mathbf{w}'). \end{aligned} \quad (197)$$

Next, if we assume that this expression is dominated by $q \sim 1/k$ we can neglect the factor $e^{i\mathbf{w}\cdot\mathbf{q}}$ in the exponent in the high- k limit $k \gg \Lambda$. Then the integration over \mathbf{q} yields the Dirac factor $\delta_D(\mathbf{w}' - \mathbf{k})$ and we obtain:

$$\delta(\mathbf{k}, D) \simeq D \delta_{L0}(\mathbf{k}) e^D \int_{w<\Lambda} d\mathbf{w} \frac{\mathbf{k}\cdot\mathbf{w}}{w^2} \delta_{L0}(\mathbf{w}). \quad (198)$$

Thus we recover eq.(193) with $D_I \rightarrow 0$ and letting $\Lambda \rightarrow \infty$. Of course, we can see that the assumptions involved in the derivation of eq.(198) from eq.(196) are identical to those involved in the derivation of eq.(193). In order to check whether these assumptions are valid we can compare the non-linear power-spectrum predicted by eq.(193) with the exact power studied in sect. 6.1. This gives (with $D_I = 0$):

$$\hat{\Delta}^2(k; D_1, D_2) = \Delta_L^2 e^{-\frac{1}{2}(D_1 - D_2)^2 k^2 \sigma_v^2}. \quad (199)$$

We can see that we again recover the exact Gaussian decay at high k for unequal times, which corresponds to the exponential term in the exact expression (112), but for equal times we merely get back the linear power Δ_L^2 . In fact, the analysis of sect. 6.2 shows that the assumptions underlying eq.(198) are not valid. Indeed, for a power-law linear power-spectrum (114) the derivation leading to eq.(117) shows that in the highly non-linear regime the non-linear power at wavenumber k is associated with scales $q \sim k^{-1+(n+3)/(n+1)}$ and with linear wavenumbers $w \sim k^{1-(n+3)/(n+1)}$. Thus, for $-3 < n < -1$ where the system is well defined we find that the power at wavenumber k is generated by linear wavenumbers w which actually grow faster than k instead of being restricted to a finite range $w < \Lambda$. Therefore, one cannot define a fixed cut-off Λ beyond which non-linear interactions are negligible so that we can expand the high- w part as in eq.(197).

Indeed, the latter integral is actually large in the non-linear regime and one needs to take into account its full non-perturbative expression to obtain the non-trivial scaling of eq.(118).

As was already clear from the linear eqs.(189), (191), the high- k approximations described above neglect the non-linear interactions associated with high wavenumbers, which actually govern the formation of large-scale structures at small scales, and only keep track of the overall displacement associated with the large-scale velocity field. This is why the low- k non-linear interactions could be resummed as $e^{-(D_1 - D_2)k^2 \sigma_v^2}$ which only involves the variance σ_v of the linear displacement field. This is clearly an important feature of the dynamics for unequal times, especially for the simple Zeldovich dynamics studied in this paper where the exact trajectories satisfy the simple law (10) and the response function (133) happens to be fully determined by this advection process. After averaging over the Gaussian initial conditions this random displacement of large-scale structures leads to an apparent ‘‘diffusion’’ in the response function in the form of a Gaussian decay $e^{-k^2 \sigma_v^2}$. However, it is actually disconnected from the building of matter clustering since as we recalled in sect. 6.2 σ_v may exhibit IR divergences without affecting equal-time clustering. This is most clearly seen from eq.(199) which shows that the diagrams of Fig. 14 do not affect the equal-time power-spectrum (in this high- k limit).

It is clear that all steps going from eq.(188) to eq.(195) can be applied identically to the exact gravitational dynamics, see Crocce & Scoccimarro (2006b). In this case we can no longer compare these approximations with exact results but eq.(199) clearly disagrees with numerical results. In particular, the previous discussion shows that in this case also the high- k approximations associated with eq.(193) do not capture the physics of gravitational clustering but only the ‘‘diffusion’’ associated with the linear velocity variance which also vanishes for equal-time statistics. Besides, since the assumptions leading to eq.(193) should again be violated, it is not obvious that the approximate response (195) should again agree with the exact response in the high- k limit, which may thus depart from such a Gaussian decay. Indeed, the small-scale gravitational dynamics is quite different from the simple Zeldovich dynamics. On the other hand, for the exact gravitational dynamics the fluid equations break down beyond shell-crossing so that the small-scale limit associated with these hydrodynamical equations is not so well defined.

10. 2PI effective action method

We now investigate the 2PI effective action method presented in sect. 4.2 and described in details in Valageas (2007). Thus, we need to solve the system of coupled equations (70)-(72) and (81)-(82). Thanks to causality, which leads to the Heaviside factor $\theta(\eta_1 - \eta_2)$ within both R and Σ , we solve this system by moving forward over time.

We refer the reader to Valageas (2007) for a description of the numerical scheme. We consider the Λ CDM cosmology associated with eq.(153) and we only investigate the one-loop predictions.

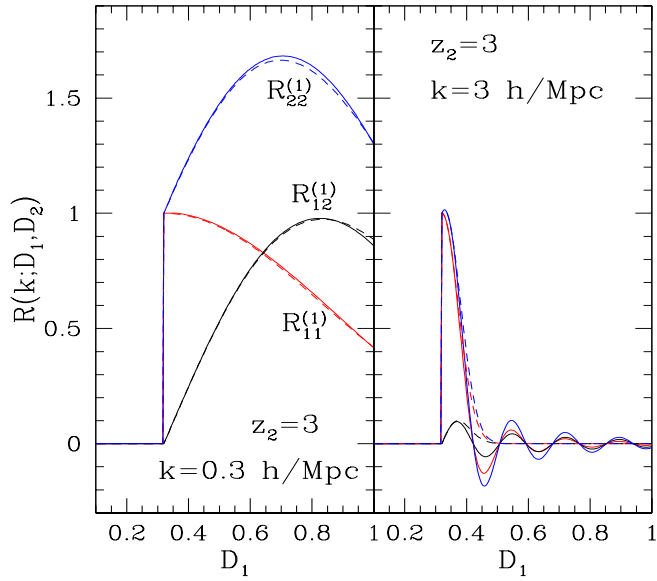


Fig. 15. The non-linear response $R(k; D_1, D_2)$ (solid lines) as a function of forward time D_1 , for $D_2 = 0.32$ (i.e. $z_2 = 3$) and wavenumbers $k = 0.3$ (left panel) and $3 \times h \text{ Mpc}^{-1}$ (right panel) for the 2PI effective action method at one-loop order. For comparison we also plot the exact response R_{NL} (dashed lines).

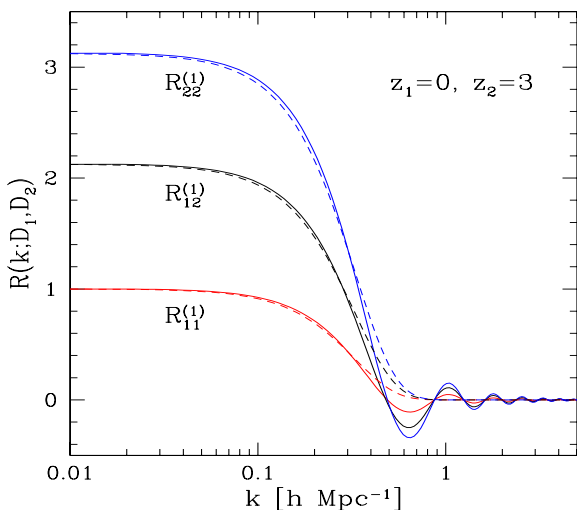


Fig. 16. The non-linear response function $R(k; D_1, D_2)$ (solid lines) as a function of wavenumber k , at times $z_1 = 0, z_2 = 3$, for the 2PI effective action method at one-loop order. We also plot the exact non-linear response R_{NL} (dashed lines).

We first display in Fig. 15 the evolution forward over time D_1 of the response $R(k; D_1, D_2)$. We can see that the non-linear response exhibits oscillations as for the steepest-descent result (163) but its amplitude now decays as an inverse power-law at large times D_1 instead of following the linear envelope (at one-loop order). As shown in sect. 6.1 of Valageas (2007) this behavior is due to the non-linearity of the Schwinger-Dyson equation for the response R . Of course, in the weakly non-linear regime we also recover the exact response (133) (dashed lines). Next, we display in Fig. 16 the response function as a function of wavenumber k . In agreement with Fig. 15, we again obtain damped oscillations in the non-linear regime. This is a clear improvement over both the standard perturbative expansion displayed in Fig. 3 and the steepest-descent result displayed in Fig. 6. This behavior is identical to the one obtained for the gravitational dynamics studied in Valageas (2007).

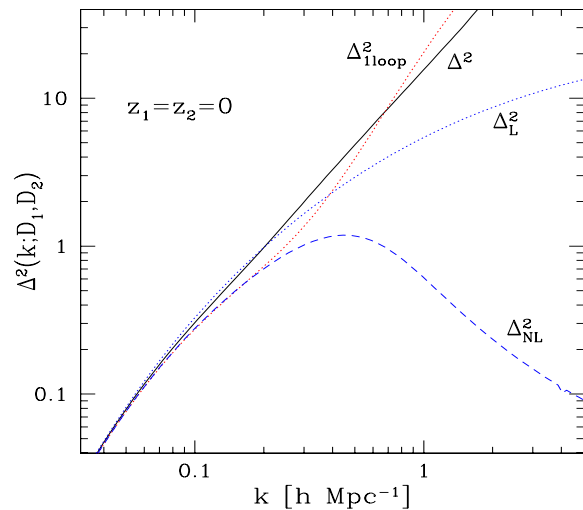


Fig. 17. The logarithmic power $\Delta^2(k)$ (solid line) at redshift $z = 0$, that is at equal times $z_1 = z_2 = 0$. We also display the linear power Δ_L^2 (dotted line), the usual one-loop perturbative result $\Delta_{1\text{loop}}^2$ of eq.(200) (dotted line) and the exact non-linear power Δ_{NL}^2 of eq.(109) (dashed line).

Finally, we show in Fig. 17 and Fig. 18 the logarithmic power $\Delta^2(k; D_1, D_2)$ as a function of wavenumber k . We compare the 2PI effective action prediction at one-loop order (solid line) with the linear power, the exact non-linear power obtained from eq.(109) and the usual one-loop result obtained from standard perturbative analysis. The latter may also be obtained by expanding eq.(109) up to order P_{L0}^2 and it reads for the Zeldovich dynamics:

$$P^{\text{1loop}}(k; D_1, D_2) = P_L + P_{22} + P_{13}, \quad (200)$$

with:

$$P_L = D_1 D_2 P_{L0}(k), \quad (201)$$

$$P_{13} = -\frac{D_1^2 + D_2^2}{2} D_1 D_2 P_{L0}(k) k^2 \sigma_v^2, \quad (202)$$

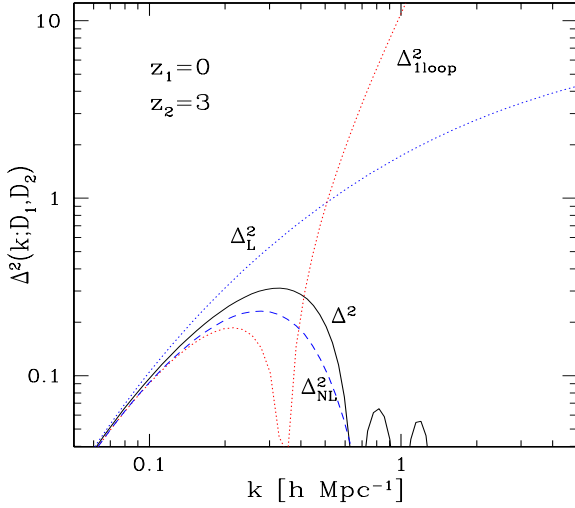


Fig. 18. The logarithmic power $\Delta^2(k)$ at unequal times ($D_1 = 1, D_2 = 0.32$) (i.e. $z_1 = 0, z_2 = 3$).

$$P_{22} = D_1^2 D_2^2 \int d\mathbf{w} \frac{(\mathbf{k} \cdot \mathbf{w})^2 [\mathbf{k} \cdot (\mathbf{k} - \mathbf{w})]^2}{2w^4 |\mathbf{k} - \mathbf{w}|^4} P_{L0}(w) P_{L0}(|\mathbf{k} - \mathbf{w}|) \quad (203)$$

The results match the steepest-descent predictions as well as the usual one-loop power (200) at large scales. At small scales, contrary to the usual one-loop power (200) and the steepest-descent predictions, the 2PI effective action method yields a logarithmic power $\Delta^2(k; D_1, D_2)$ which decays for different times $D_1 \neq D_2$, see Fig. 18. This high- k power-law damping is due to the decay of the response function already shown in Fig. 15 and Fig. 16, leading to a decorrelation at small scales and large time separations. Note however that is only a power-law decay instead of the exact Gaussian damping seen in eq.(112). On the other hand, for equal times $D_1 = D_2 = D$ we obtain a steady growth of the power $\Delta^2(k)$ in between the linear prediction Δ_L^2 and the usual one-loop prediction $\Delta_{1\text{loop}}^2$, see Fig. 17. This is due to the contributions of nearby times $D'_1 \simeq D'_2 \simeq D$ in the last term of eq.(83) which are not damped because of their small time-difference. Note that the cancellation at equal times of the damping associated with the decay of the response function is qualitatively correct, as shown from the exact non-linear solution studied in sects. 6.1, 6.2, see eq.(112). Therefore, at one-loop order the 2PI effective action method shows a significant qualitative improvement over the standard perturbative expansions of sect. 7 and the direct steepest-descent method. However, it does not manage to predict the high- k smooth power-law decay of the equal-time power $\Delta^2(k)$.

11. Simple non-linear schemes associated with the 2PI effective action method

11.1. Response function

For the 2PI effective action method it is not straightforward to obtain the self-energy Σ at a given order from the

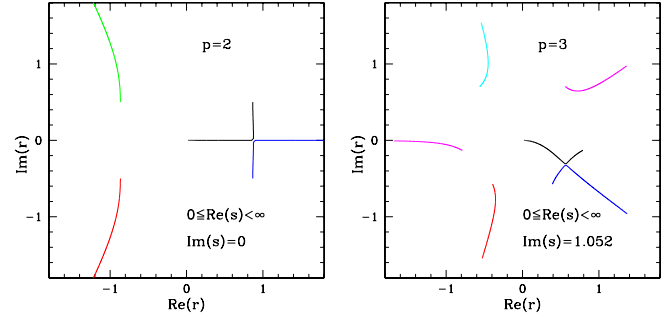


Fig. 19. *Left panel:* the trajectories of the four roots of eq.(211) as we follow s along the real axis from $s = +\infty$ down to $s = 0$. *Right panel:* the trajectories of the six roots of eq.(212) as we follow s along the line $\text{Im}(s) = 1.052$ from $\text{Re}(s) = +\infty$ down to $\text{Re}(s) = 0$. The root of interest starting from $\tilde{r} = 0$ “collides” with a second root and makes a change of direction by $\pi/2$. This corresponds to a singularity for the implicit function $\tilde{r}(s)$.

exact expressions (140) or (142). Indeed, for the steepest-descent approach investigated in sect. 8 the self-energy at a given order simply corresponds to the truncation of its expansion over powers of P_{L0} . Therefore, it could be directly obtained by expanding the exact result. By contrast, within the 2PI effective action scheme the self-energy is obtained from a diagrammatic expansion in terms of the non-linear response R and correlation G (defined self-consistently at this order). Then, the exact expressions of the response R and correlation G are not sufficient to fully define the equations associated with the 2PI effective action method at any order and one must go back to its diagrammatic definition. To avoid this complication so as to take advantage of the known expressions of the exact two-point functions, which allowed us to bypass the computation of high-order diagrams in sect. 8, we investigate here a non-linear expansion which is not identical to the 2PI effective action but is expected to share a similar behavior. Thus, we look for an expansion of the self-energy Σ over the non-linear response R . A simple way to build such an expansion is to use the expansions over $1/s$ of the Laplace transforms $\tilde{r}(s)$ and $\tilde{\sigma}(s)$. Thus, from eq.(164) and the Laplace transform of eq.(142), we have:

$$\tilde{r}(s) = \frac{1}{s} - \frac{1}{s^3} + \frac{3}{s^5} - \frac{15}{s^7} + \frac{105}{s^9} + \dots \quad (204)$$

$$\tilde{\sigma}(s) = \frac{1}{s} - \frac{2}{s^3} + \frac{10}{s^5} - \frac{74}{s^7} + \frac{706}{s^9} + \dots \quad (205)$$

Then, the series (204) may be inverted as:

$$\frac{1}{s} = \tilde{r} + \tilde{r}^3 + 3\tilde{r}^7 - 20\tilde{r}^9 + \dots \quad (206)$$

Composing this expansion with eq.(205) we obtain:

$$\tilde{\sigma} = \tilde{r} - \tilde{r}^3 + 4\tilde{r}^5 - 27\tilde{r}^7 + 248\tilde{r}^9 + \dots \quad (207)$$

This provides an expansion of the self-energy Σ in terms of the non-linear response R . In real t -space this yields multiple integrals over $r(t)$:

$$\sigma(t) = r(t) - \int_0^t dt_1 \int_0^{t_1} dt_2 r(t-t_1)r(t_1-t_2)r(t_2) + \dots \quad (208)$$

in a fashion similar to what would be obtained for the diagrammatic expansion associated with the 2PI effective action. The main difference is that the expansion (207) only involves the response R whereas the 2PI effective action expansion involves both R and G , as in eq.(81). Note that this shows that one can define several non-linear expansion schemes. The fact that it is possible to write a simple expansion such as (207) is due to the fact that the exact response R only depends on the linear power-spectrum through the velocity dispersion σ_v^2 . This is not the case for the gravitational dynamics where it may not be possible to write an expansion for Σ in terms of R only. Next, truncating the expansion (207) at a given order and substituting into eq.(136), we obtain at order $p = 1$:

$$\tilde{\sigma} = \tilde{r}, \quad \tilde{r}^2 + s\tilde{r} - 1 = 0, \quad \tilde{r}^{(1)}(s) = \frac{\sqrt{s^2 + 4} - s}{2}. \quad (209)$$

The root of the polynomial of degree $2p$ which must be chosen is the one which is consistent with the expansion (204) for $s \rightarrow \infty$. Eq.(209) is a well-known Laplace transform and we obtain:

$$r^{(1)}(t) = \frac{J_1(2t)}{t}. \quad (210)$$

Note that this expression was also obtained as a simple approximation for the one-loop 2PI effective action approach for the gravitational dynamics in Valageas (2007). We also recover the damped oscillations obtained within the 2PI effective action method displayed in Figs. 15, 16. Thus, as expected this non-linear expansion and the 2PI effective action expansion show the same behavior at order $p = 1$. At orders $p = 2, 3$ we obtain the polynomial equations:

$$p = 2 : -\tilde{r}^4 + \tilde{r}^2 + s\tilde{r} - 1 = 0 \quad (211)$$

$$p = 3 : 4\tilde{r}^6 - \tilde{r}^4 + \tilde{r}^2 + s\tilde{r} - 1 = 0 \quad (212)$$

However, we now find that the solutions $\tilde{r}^{(p)}(s)$ defined from these equations have singularities in the right-hand half-plane $\text{Re}(s) > 0$. For order $p = 2$ this may be directly seen from the explicit solution of eq.(211) or from the behavior of the four roots $\tilde{r}_i(s)$ as a function of s shown in left panel of Fig. 19. Indeed, we see that as we follow s along the real axis from $+\infty$ to 0 the root of interest $\tilde{r}_1(s)$ which starts from $\tilde{r}_1 = 0$ at $s = +\infty$ ‘‘collides’’ with a second root \tilde{r}_2 at $\tilde{r}_* \simeq 0.87$ ($s_* \simeq 0.94$) and afterwards forms a pair of complex conjugates with \tilde{r}_2 . This is associated with a square-root singularity for $\tilde{r}(s)$ (a simple example is provided by the polynomial $\tilde{r}^2 - s = 0$ with a singularity at $\tilde{r}_* = 0, s_* = 0$). For order $p = 3$, the right panel of Fig. 19 where we follow s along the line $\text{Im}(s) = 1.052$ from $\text{Re}(s) = +\infty$ down to $\text{Re}(s) = 0$

shows that we again have a singularity at the complex points $s_* \simeq 1.17 \pm 1.05i, \tilde{r}_* \simeq 0.56 \mp 0.31i$. These singularities yield exponential factors e^{s_*t} for the response $r(t)$ which grow at large t . Therefore, although the expansion (207) is much better than the steepest-descent approach (163) at order $p = 1$, since it exhibits a damping in the non-linear regime, it shows as for expansion (163) growing exponentials at higher orders. Thus, in this sense this non-linear expansion is not well behaved. We can expect that a similar problem occurs for the 2PI effective action approach at high orders.

11.2. Correlation function

We now investigate non-linear schemes for the two-point correlation G . As for the response function we look for a simple non-linear expansion which bypasses the need to compute high-order diagrams but which follows the structure of the 2PI effective action method. This is not as straightforward as for the response R because the two-point correlation G cannot be written in terms of a one-dimensional function such as $r(t)$ for the response R . Thus, we focus on the equal-time non-linear power for the case of a power-law linear power-spectrum and we write:

$$\Delta^2(k; D) = \Delta_L^2 g(t) \quad \text{with} \quad t = D\sqrt{\Delta_{L0}^2} = \sqrt{\Delta_L^2} \quad (213)$$

which defines the time-variable t used in this section and the function $g(t)$. From eq.(156) and eq.(175) we have for $n = -2$:

$$g(t) = \sum_{p=1}^{\infty} \frac{F_p}{p!} t^{2p-2}, \quad (214)$$

which yields for the Laplace transform defined as in eq.(137):

$$\tilde{g}(s) = \sum_{p=1}^{\infty} \frac{F_p}{p!} (2p-2)! s^{-2p+1} = \frac{1}{s} + \frac{3\pi^2}{32s^3} - \frac{3\pi^2}{4s^5} + \dots \quad (215)$$

This series can be inverted as:

$$\frac{1}{s} = \tilde{g} - \frac{3\pi^2}{32}\tilde{g}^3 + \frac{3(256\pi^2 + 9\pi^4)}{1024}\tilde{g}^5 + \dots \quad (216)$$

Next, the derivative of $g(t)$ verifies:

$$g'(t) = \sum_{p=2}^{\infty} \frac{F_p}{p!} (2p-2) t^{2p-3} \quad (217)$$

and the Laplace transform of this equation reads:

$$\begin{aligned} s\tilde{g}(s) - 1 &= \sum_{p=2}^{\infty} \frac{F_p}{p!} (2p-2)! s^{-2p+2} \\ &= \frac{3\pi^2}{32s^2} - \frac{3\pi^2}{4s^4} - \frac{675\pi^4}{512s^6} + \dots \end{aligned} \quad (218)$$

which could also be obtained from eq.(215). Then, substituting the series (216) into eq.(218) gives:

$$s\tilde{g}(s) - 1 = \frac{3\pi^2}{32}\tilde{g}^2 - \frac{3\pi^2(128 + 3\pi^2)}{512}\tilde{g}^4 + \dots \quad (219)$$

Thus, as for the response function studied in sect. 11.1, we have obtained a simple non-linear expansion scheme for the two-point correlation G (i.e. for the non-linear power $\Delta^2(k; D)$). However, since the functional dependence of the two-point correlation G is not as simple as for the response R the expansion (219) only applies to the equal-time power and it is not built from the self-energy Π . Nevertheless, going back to real t -space eq.(219) yields an integro-differential equation for G such as eq.(70), with a fixed differential term in the l.h.s. and a series of multiple integrals over $g(t)$ in the r.h.s. At order $p = 0$ the r.h.s. is zero and we recover the linear solution $g^{(0)}(t) = 1$. At order $p = 1$ we obtain:

$$s\tilde{g} - 1 = \frac{3\pi^2}{32}\tilde{g}^2, \quad \tilde{g}^{(1)}(s) = \frac{16}{3\pi^2} \left[s - \sqrt{s^2 - 3\pi^2/8} \right], \quad (220)$$

which gives:

$$g^{(1)}(t) = \sqrt{\frac{2}{3}} \frac{4}{\pi t} I_1 \left(\sqrt{\frac{3}{2}} \frac{\pi t}{2} \right), \quad (221)$$

where I_1 is the modified Bessel function of order 1. Thus, the non-linear power $\Delta^{2(1)}$ shows an exponential growth in the highly non-linear regime. We can check that at order $p = 2$ we again have an exponential growth (with oscillations since $\text{Im}(s_*) \neq 0$ where s_* is the location of the singularity of $\tilde{g}^{(2)}(s)$). Therefore, the non-linear expansion (219) is not better behaved than the ‘‘linear’’ expansions associated with the steepest-descent approach studied in sect. 8.3.

12. Simple non-linear schemes associated with the running with the high- k cutoff

12.1. Response function

In a fashion similar to sect. 11, we now investigate some non-linear schemes which may be built in the spirit of the method outlined in sect. 5, where we considered the dependence of the system on a high- k cutoff Λ . In order to separate the dependence on Λ we now write the response function as:

$$R = R_L r(t, \omega^2) \quad \text{with} \quad t = D_1 - D_2, \quad (222)$$

$$\omega^2 = k^2 \frac{4\pi}{3} \int_0^\Lambda dw P_{L0}(w). \quad (223)$$

Thus, the exact response function $r(t, \omega^2)$ is from eq.(133):

$$r(t, \omega^2) = e^{-\omega^2 t^2/2}. \quad (224)$$

Defining the Laplace transform with respect to t as in eq.(137) we obtain:

$$\tilde{r}(s, \omega^2) = \sum_{p=0}^{\infty} (-1)^p (2p-1)!! \omega^{2p} s^{-2p-1} \quad (225)$$

while the derivative with respect to Λ is:

$$\frac{\partial \tilde{r}}{\partial \Lambda}(s, \omega^2) = \frac{d\omega^2}{d\Lambda} \sum_{p=1}^{\infty} (-1)^p (2p-1)!! p \omega^{2(p-1)} s^{-2p-1} \quad (226)$$

Inverting the series (225) and substituting into eq.(226) gives the expansion:

$$\frac{\partial \tilde{r}}{\partial \Lambda} = \frac{d\omega^2}{d\Lambda} [-\tilde{r}^3 + 3\omega^2 \tilde{r}^5 - 18\omega^4 \tilde{r}^7 + \dots] \quad (227)$$

At order $p = 0$ we have $\partial \tilde{r}/\partial \Lambda = 0$ and we recover the linear response (since we impose $r(\Lambda = 0) = r_L$). At order $p = 1$ we obtain:

$$\frac{\partial \tilde{r}}{\partial \Lambda} = -\frac{d\omega^2}{d\Lambda} \tilde{r}^3 \quad (228)$$

which is similar to eq.(91) once we go back to real t -space which leads to a double integral over time (as in eq.(208)). We can recover eq.(92) by noting that the linear response is $\tilde{r}_L(s) = 1/s$ whence $\tilde{r}_L^3 = 1/2d^2\tilde{r}_L/ds^2$ and substituting this result into eq.(228) gives $\partial \tilde{r}/\partial \Lambda = -1/2(d\omega^2/d\Lambda)d^2\tilde{r}_L/ds^2$. The inverse Laplace transform of this equation gives back eq.(92). It is clear that this procedure is not systematic and only applies to the linear response. This is why we could reduce the three response functions in the r.h.s. of eq.(91) to the one response function in the r.h.s. of eq.(92). Then, replacing R_L by R in eq.(92) is clearly correct at the order ω^2 at which the r.h.s. of eq.(90) was truncated but this method cannot be extended to higher orders in a systematic fashion. Thus, let us consider eq.(228) with keeping the r.h.s. as it comes out from the systematic expansion obtained in (227). Integrating over Λ gives:

$$\tilde{r}^{(1)}(s) = \frac{1}{\sqrt{s^2 + 2\omega^2}} \quad \text{whence} \quad r^{(1)}(t) = J_0(\sqrt{2}\omega t). \quad (229)$$

Thus, we obtain decaying oscillations into the non-linear regime which are damped as $[k(D_1 - D_2)]^{-1/2}$. Note that the damping is smaller than for the 2PI effective action method where the simplified expansion (207) gave eq.(210) which decays as $[k(D_1 - D_2)]^{-3/2}$. At next order $p = 2$ we obtain:

$$\frac{\partial \tilde{r}}{\partial \Lambda} = \frac{d\omega^2}{d\Lambda} [-\tilde{r}^3 + 3\omega^2 \tilde{r}^5] \quad \text{hence} \quad \frac{\partial \tilde{r}}{\partial \omega^2} = -\tilde{r}^3 + 3\omega^2 \tilde{r}^5 \quad (230)$$

Then, looking for a solution of the form:

$$r(t, \omega^2) = \rho(\omega t), \quad \tilde{r}(s, \omega^2) = \frac{1}{\omega} \tilde{\rho}(y) \quad \text{with} \quad y = \frac{s}{\omega}, \quad (231)$$

we obtain for the Laplace transform $\tilde{\rho}(y)$ the equation:

$$\tilde{\rho} + y\tilde{\rho}' = 2\tilde{\rho}^3 - 6\tilde{\rho}^5. \quad (232)$$

Note that eq.(232) no longer involves an explicit dependence on ω . It can be solved in implicit form as:

$$y = \frac{1}{\tilde{\rho}} (1 - 2\tilde{\rho}^2 + 6\tilde{\rho}^4)^{1/4} e^{[\arctan \sqrt{5} - \arctan(\frac{\sqrt{5}}{1-6\tilde{\rho}^2})]} / (2\sqrt{5}) \quad (233)$$

Going back to $s = \omega y$ we see that $\tilde{r}(s, \omega^2)$ is singular at the point:

$$s_* = \omega y_* \quad \text{with} \quad y_* = 6^{1/4} e^{\frac{1}{2\sqrt{5}} \arctan \sqrt{5}}, \quad s_* > 0, \quad (234)$$

where $|\tilde{r}| = \infty$. Therefore, the response function obtained at order $p = 2$ grows into the non-linear regime

as $r^{(2)} \sim e^{s^*t}$ which gives $R^{(2)} \sim e^{y_*k\sigma_v(D_1-D_2)}$. Thus, as for the non-linear scheme of sect. 11.1 associated with the 2PI effective action method we find that at high orders the expansion (227) gives rise to response functions which exhibit an exponential growth into the non-linear regime, even though at lowest-order $p = 1$ it managed to provide a non-linear damping. Therefore, the fact that the Gaussian decay could be recovered from eq.(92) is not due to the good convergence properties of the method outlined in sect. 5. As discussed in sect. 5 from eq.(94) it merely comes from the successive steps which have been performed using the properties of the linear response until one gets the linear eq.(92), which is correct at lowest order and which has the desired solution. However, these intermediate steps cannot be directly extended to high orders without ambiguities and the systematic non-linear expansion (227) does not recover this damping at high orders.

12.2. Correlation function

For the correlation function G , following the procedure of sect. 11.2 and sect. 12.1, we write:

$$\Delta^2(k; D) = \Delta_L^2 g(t, \Delta_{L0}^2) \quad \text{with} \quad t = D. \quad (235)$$

Then, introducing again the Laplace transform with respect to t , inverting the series $\tilde{g}(s, \Delta_{L0}^2) = 1/s + \dots$ and substituting into $\partial\tilde{g}/\partial\Lambda$ gives the expansion:

$$\frac{\partial\tilde{g}}{\partial\Lambda} = \frac{d\Delta_{L0}^2}{d\Lambda} \left[\frac{3\pi^2}{32}\tilde{g}^3 - \frac{3\pi^2(512+9\pi^2)}{1024}\Delta_{L0}^2\tilde{g}^5 + \dots \right] \quad (236)$$

At order $p = 0$ we have the linear correlation $\partial\tilde{g}/\partial\Lambda = 0$, $\tilde{g} = 1/s$ and $g(t) = 1$. At order $p = 1$ we obtain:

$$\frac{\partial\tilde{g}}{\partial\Delta_{L0}^2} = \frac{3\pi^2}{32}\tilde{g}^3, \quad \tilde{g}^{(1)}(s) = \frac{1}{\sqrt{s^2 - 3\pi^2\Delta_{L0}^2/16}}, \quad (237)$$

which gives:

$$g^{(1)}(t, \Delta_{L0}^2) = I_0 \left(\frac{\sqrt{3}\pi}{4}\Delta_{L0}t \right), \quad (238)$$

where I_0 is the modified Bessel function of order 0. Thus, as for the simple non-linear scheme associated with the 2PI effective action method of sect. 11.2, we obtain at order $p = 1$ a non-linear equal-time power Δ^2 which shows an exponential growth in the non-linear regime. Following the method leading to eq.(233) we can actually integrate the non-linear equation (236) at any order, using the scaling $\tilde{g}(s, \Delta_{L0}^2) = \tilde{\gamma}(s/\Delta_{L0})/\Delta_{L0}$ which transforms eq.(236) into an implicit equation giving $y = s/\Delta_{L0}$ as the integral of a rational function of $\tilde{\gamma}$. We can check that at order $p = 2$ we again have an exponential growth into the non-linear regime (with oscillations because $\text{Im}(y_*) \neq 0$).

13. Weakly non-linear scales

In the previous sections we have investigated the convergence properties of several expansion schemes which

may be used to study gravitational clustering in the expanding Universe, applied to the case of the Zeldovich dynamics where exact results can be obtained. In this section, we complete this study by a brief description of the results obtained at one-loop order on weakly non-linear scales. Indeed, an accurate prediction for the matter power-spectrum on these scales is of great practical interest for several cosmological probes such as baryonic acoustic oscillations (Eisenstein et al. 1998, 2005) and weak-lensing shear (Munshi et al. 2007). For the exact gravitational dynamics the various expansion schemes must be compared with numerical simulations which is not very convenient to discriminate their power. Therefore, it is interesting to check against the Zeldovich dynamics the accuracy and the behavior of these expansion methods.

13.1. Linear expansion schemes

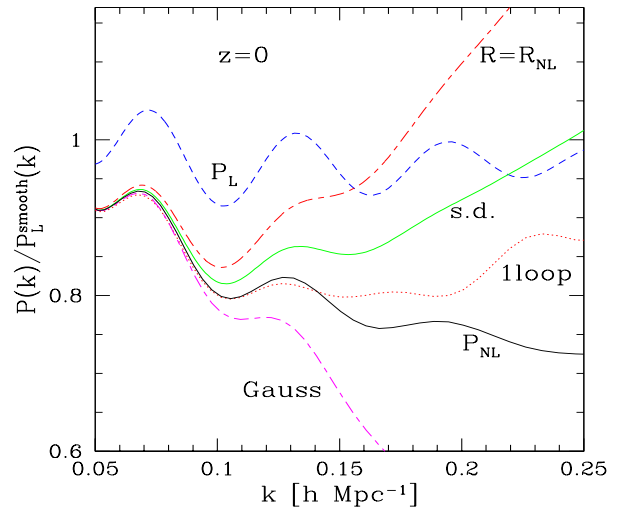


Fig. 20. The power-spectrum $P(k)$ divided by a smooth linear power P_L^{smooth} at redshift $z = 0$. We display the linear power $P_L(k)$ (dashed line), the exact non-linear power P_{NL} of eq.(109), the standard 1-loop result (dotted line) of eq.(200) and the steepest-descent result of eq.(83) (upper solid line “s.d.”). We also show the results obtained by adding a Gaussian factor to the standard perturbative result as in eq.(159) (lower dot-dashed line) or by using the exact non-linear response R_{NL} in eq.(83) within the steepest-descent scheme (upper dashed line), as in Fig. 10.

We first consider “linear” expansion schemes, that is methods which give rise to expansions in terms of the linear power-spectrum, such as the standard perturbative expansions of sect. 7 and the direct steepest-descent methods of sect. 8. We focus on the equal-time power spectrum for the Λ CDM universe described in the first paragraph of sect. 7. We use the CAMB Boltzmann code (Lewis et al. 2000) to obtain the linear power-spectrum with the baryonic acoustic oscillations. In order to magnify the difference between various schemes we show in Figs. 20, 21

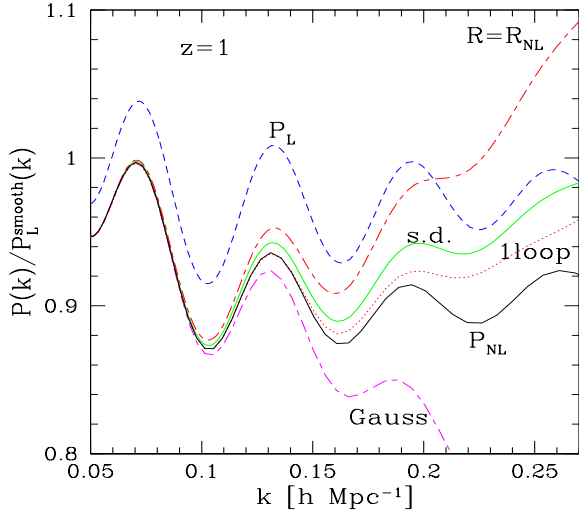


Fig. 21. The power-spectrum $P(k)$ divided by a smooth linear power P_L^{smooth} as in Fig. 20, but at redshift $z = 1$.

the non-linear power divided by the linear power P_L^{smooth} associated to a smooth power-spectrum without baryonic oscillations, taken from Eisenstein & Hu (1998). First, we see in Fig. 20 that all schemes agree with the exact power up to $k \simeq 0.1 h \text{ Mpc}^{-1}$ at redshift $z = 0$ and they follow the departure from the linear power P_L . At smaller scales the various expansion schemes deviate from each other and from the exact non-linear power. It is interesting to note that using the exact non-linear response (133) within the steepest-descent scheme (upper dashed line) does not improve the agreement over the original steepest-descent scheme (labeled “s.d.”) where we use the response function predicted at the same order. On the other hand, it appears that the standard one-loop expansion provides the best results at this order.

Following eq.(159) and Fig. 5 we also consider the expansion defined from the standard perturbative series by factorizing a Gaussian decay:

$$\begin{aligned} P_{\text{Gauss.}}^{\text{1loop}}(k) &= e^{-D^2\omega^2} [P_L + P_{22} + P_{13} + D^2\omega^2 P_L] \\ &= e^{-D^2\omega^2} (P_L + P_{22}). \end{aligned} \quad (239)$$

In agreement with sect. 7 and Crocce & Scoccimarro (2006a) we can note that this gives a positive power whatever the shape of the linear power-spectrum. However, Fig. 20 shows that this does not necessarily improve the accuracy as compared with the usual one-loop result (200). We show in Fig. 21 the power-spectrum obtained at redshift $z = 1$. Of course the various expansion schemes agree more closely on the same scales with the exact result since we are closer to the linear regime. We can see that we recover the same behaviors as in Fig. 20.

13.2. Non-linear expansion schemes

Finally, we study in this section “non-linear” expansion schemes, that is methods which give rise to expansions in

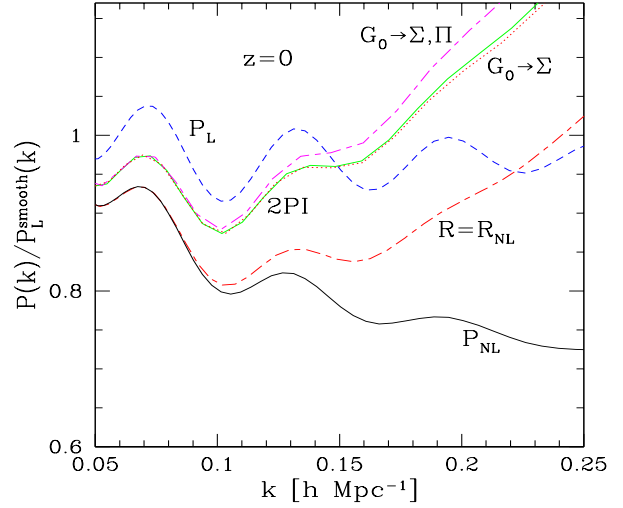


Fig. 22. The power-spectrum $P(k)$ divided by a smooth linear power P_L^{smooth} at redshift $z = 0$. We display the linear power $P_L(k)$ (dashed line), the exact non-linear power P_{NL} of eq.(109), and the 2PI effective action result of eq.(83) (upper solid line “2PI”). We also show the results obtained by using the exact non-linear response R_{NL} in eq.(83) within the 2PI scheme (lower dashed line), or by using the linear two-point correlation to compute both Σ and Π (upper dot-dashed line) or only Σ (dotted line).

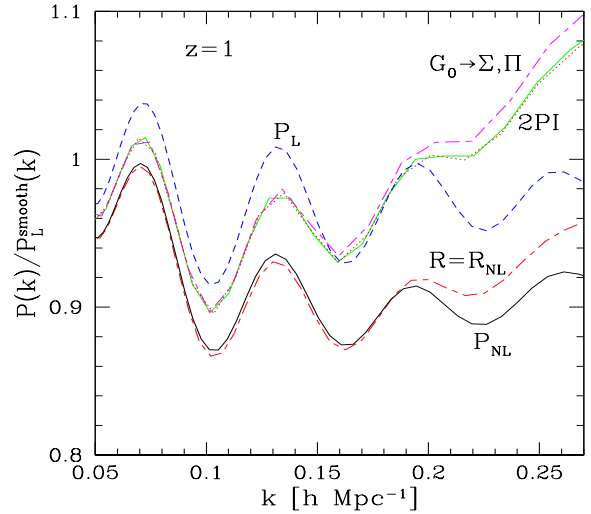


Fig. 23. The power-spectrum $P(k)$ divided by a smooth linear power P_L^{smooth} as in Fig. 22, but at redshift $z = 1$.

terms of the non-linear two-point functions R and G , such as the 2PI effective action method of sect. 4.2 and sect. 10. We show our results for the power-spectrum (divided again by P_L^{smooth}) at redshifts $z = 0, 1$ in Figs. 22, 23. First, we note that the 2PI effective action result at one-loop order overestimates the power-spectrum on weakly non-linear scales. Both the standard one-loop result and the direct steepest-descent method actually work better in this range. This behavior can be traced back to the

damping self-energy Σ . Indeed, since $\Sigma \propto RG$ at one-loop order, see eq.(81), the decay of the response and of the two-point correlation at high k (shown in Fig. 16 and Fig. 18) leads to a smaller $\Sigma(k)$ at high k as compared with Σ_0 obtained for the direct steepest-descent method. This in turn yields a response R which is somewhat larger than for the steepest-descent method in the weakly non-linear regime (but smaller at high k where it decays) whence a two-point correlation G which is somewhat larger from eq.(83). Of course, this slight overestimate of R and underestimate of Σ will be corrected by higher-order terms. In particular, for the Zeldovich dynamics we know that R and Σ actually only depend on σ_v so that terms which depend on other integrals over $P_{L0}(k)$ must cancel out in the full resummation. However, this discrepancy makes the one-loop 2PI effective action result insufficient for practical purposes (at least at the one-loop order).

We also display the results obtained when both the self-energies Σ and Π are obtained from the linear correlation G_0 (upper dot-dashed line, so that only the response R coupled to Σ is obtained from non-linear equations) and when only the self-energy Σ is obtained from G_0 (upper dotted line, so that the non-linear systems for the pairs $\{\Sigma, R\}$ and $\{\Pi, G\}$ are decoupled). We see that these two methods give results very close to the original 2PI effective action prediction where all two-point functions $\{\Sigma, \Pi, R, G\}$ are coupled.

On the other hand, we also show the power-spectrum obtained from the coupled equations (82) and (83) when we use the exact non-linear response (133). We can see that this significantly improves the agreement with the exact power-spectrum and the result is slightly better than the steepest-descent prediction shown in Fig. 20 but it is still a bit less accurate than the standard perturbative result at $z = 0$. However, Fig. 23 shows that at $z = 1$ the power obtained in this fashion is slightly more accurate than the standard perturbative result. Therefore, contrary to the case of the steepest-descent method studied in sect. 13.1, using the exact non-linear response improves the prediction for the two-point correlation and provides a scheme which can be competitive with the usual perturbative expansion on weakly non-linear scales.

14. Conclusion

In this article we have studied for the simple case of the Zeldovich dynamics various expansion schemes which may be applied to the gravitational dynamics in the expanding Universe. Indeed, the equations of motion are very similar as they take the form of a stochastic quadratic evolution equation for a two-component field. Moreover, they only differ through the linear term and they admit the same linear growing mode. Then, we have derived the path-integral formalism which describes this system. We have shown how this can be obtained from either the differential or integral form of the equations of motion and we have derived the relationship between the response functions obtained in both cases. These response functions describe

the response of the system to a small perturbation applied at any time and they also encode the memory of initial conditions. Next, we have briefly described how to build various expansion schemes from these path-integral, such as large- N expansions or running with a high- k cutoff. Note that all these results apply almost identically to the case of the gravitational dynamics.

Then, we have derived the exact non-linear two-point functions associated with the Zeldovich dynamics taking advantage of the well-known exact solution of the equations of motion. We have noticed that different-time two-point functions, such as the response $R(k; t_1, t_2)$ or the correlation $G(k; t_1, t_2)$ show a Gaussian decay $e^{-k^2 \sigma_v^2 (D_1 - D_2)^2 / 2}$, where σ_v is the variance of the linear velocity (proportional to the displacement field). This ‘‘diffusive’’ damping is associated with the displacement of particles between different times but it is not directly related to the matter clustering. Indeed, the linear velocity variance σ_v^2 can be made very large and even infinite through low- k divergences (if $kP_L(k) \rightarrow \infty$ for $k \rightarrow 0$) without affecting the equal-time matter power spectrum $P(k; t)$. It is well-known that this cancellation of IR divergences is due to Galilean invariance (Vishniac 1983; Jain & Bertschinger 1996). This also means that the matter power-spectrum $P(k; t)$ may still be very close to linear at scale k even though two-point functions such as $R(k; t_1, t_2)$ may already show large deviations from their linear values at the same scale and previous times $t_2 < t_1 < t$. Therefore, departures from linearity of different two-point functions are not necessarily related. On the other hand, for a power-law linear power-spectrum the equal-time non-linear logarithmic power $\Delta^2(k; t) \propto k^3 P(k; t)$ only decays as a power-law in the highly non-linear regime.

Next, we have studied the standard perturbative expansions for both the response R and the power Δ^2 , focussing on a power-law linear power-spectrum $n = -2$ for the latter. The usual perturbative expansion being equivalent to a Taylor expansion it cannot capture the different-time Gaussian decay of R and Δ^2 nor the equal-time power-law decay of Δ^2 since it gives polynomial approximations of increasing order. In the spirit of Crocce & Scoccimarro (2006a), we noticed that for the power Δ^2 reorganizing the perturbative series by factorizing a simple Gaussian term $e^{-D^2 k^2 \sigma_v^2}$ gives an expansion which looks better behaved as all terms become positive and there is a Gaussian damping. However, this procedure only works for linear power-spectra such that the scales which govern σ_v^2 and Δ^2 are close. Clearly, adding some power at low k (e.g. through an extended $1/k$ tail) so as to make σ_v^2 very large without affecting matter clustering would make this procedure even worse than the standard perturbative expansion. Fortunately, for typical Λ CDM matter power-spectra (which are curved with n going from 1 to -3 from low k to high k and where $n \simeq -1$ close to transition to non-linearity at $z = 0$) this problem does not occur, but this argument shows that the improvement associated with this reorganization is not guaranteed.

Then, we have studied the steepest-descent method derived from a large- N expansion. We have found that at first order $p = 1$ there is some improvement for the response function which remains bounded (as a cosine) instead of growing as k^2 . The same behavior is obtained for the gravitational dynamics (Valageas 2007). However, at higher orders the expansion worsens as it exhibits an exponential growth into the non-linear regime. We have shown that this could be cured by using Padé approximants which remain bounded at all orders as a sum of cosines (they do not decay but after integration the oscillations should produce some effective damping). Then, the power Δ^2 displays an exponential growth at orders $p \geq 2$ for the plain steepest-descent method and a polynomial growth using the Padé approximants. As for the standard perturbative expansion, one can reorganize the series by factorizing a Gaussian term $e^{-(D_1^2 + D_2^2)k^2 \sigma_v^2/2}$ in the self-energy Π which describes the generation of power by non-linear interactions. This appears to give slightly better results than with the standard perturbative expansion but this procedure obviously suffers from the same restrictions. Alternatively, one can factorize a Gaussian term such as $e^{-(D_1^2 - D_2^2)k^2 \sigma_v^2/2}$ into the self-energy Π to reproduce the fact that the Gaussian damping must disappear for equal-time statistics. Then, one obtains again a polynomial growth into the highly non-linear regime for the power $\Delta^2(k; t)$ because of the contribution of recent mode couplings at times $t_1 \simeq t_2 \simeq t$. Therefore, none of these methods shows very satisfactory global convergence properties.

Next, we have discussed a high- k resummation proposed by Crocce & Scoccimarro (2006b) to improve the behavior of such expansion schemes. Indeed, performing a partial resummation of the standard perturbative diagrams they managed to recover the Gaussian decay of the response function (which happens to be exact for the Zeldovich dynamics but should only be approximate for the gravitational dynamics where there could be additional prefactors or even a non-Gaussian decay). Then, using this result for the response function one could improve the predictions for the power-spectrum as discussed above. We have shown that the partial resummation involved in this procedure is actually equivalent to approximating the non-linear equation of motion by a linear equation. Besides, using the high- k asymptotic of the coupling kernel, as in Crocce & Scoccimarro (2006b), we derived the explicit expression of the non-linear density field $\delta(\mathbf{x}, t)$ associated with these approximations. We recover in this fashion the Gaussian decay of the response function and we note that the non-linear power-spectrum implied by these approximations is actually equal to the linear power multiplied by the same different-time Gaussian decay. Therefore, the diagrams involved in this resummation describe the apparent ‘‘diffusion’’ between different times (after averaging over the Gaussian initial conditions) but they do not give information on the actual clustering of matter.

Thus, we find that these approximations manage to capture the different-time Gaussian decay but they fail to capture the equal-time properties of the system. Indeed, a close analysis of this procedure shows that the underlying assumptions are not valid because one cannot define a high- k limit in a simple manner. Thus, for a linear power-spectrum with $-3 < n < -1$ at high k (i.e. without a strong high- k cutoff) the non-linear power at wavenumber k is generated by the highly non-linear couplings of modes $k' \gg k$ instead of being produced by small wavenumbers restricted to some finite range $k' < \Lambda$. The same caveats should apply to the gravitational dynamics, although it is not totally obvious whether the Gaussian decay at different times is exact in this case (but this is not necessarily important for practical purposes).

Then, we have turned to non-linear schemes, that is expansions over powers of non-linear two-point functions, such as the 2PI effective action method built from a large- N expansion. Since it gives a system of non-linear equations which cannot be solved analytically we have presented a numerical computation at one-loop order ($p = 1$). We now obtain damped oscillations (with a power-law decay) for the two-time response function and power $\Delta^2(k; t_1, t_2)$ but the equal-time power still grows at small scales. Note that one obtains the same behavior for the gravitational dynamics (Valageas 2007). Then, from the exact two-point functions we built simple non-linear expansion schemes which are similar to the 2PI effective action expansion but can be more easily handled analytically. We recover damped oscillations for the response function at order $p = 1$ but we find an exponential growth at higher orders. On the other hand, the equal-time power also shows an exponential growth. Next, we investigated simple non-linear expansion schemes associated with the evolution of the system with a high- k cutoff Λ . We found a similar behavior as we again obtain damped oscillations at order $p = 1$ and exponential growth at higher orders for the response function as well as exponential growth for the equal-time power. In particular, we point out that in order to recover the Gaussian decay from the expansion at order $p = 1$ one must introduce some further approximations, as in Matarrese & Pietroni (2007), which are correct at this order but which do not give a systematic procedure. Therefore, it appears that at high orders $p \geq 2$ non-linear methods do not fare much better than linear schemes.

Finally, we have studied the quantitative predictions of these various schemes at one-loop order on weakly non-linear scales for the equal-time matter power-spectrum. We have checked that all linear expansions agree with the exact results on quasi-linear scales ($k < 0.1h \text{ Mpc}^{-1}$ at $z = 0$) where there is already a deviation of 10% from linear theory. At smaller scales they depart from each other and it appears that the standard perturbation theory actually works best for the case studied in this article. Moreover, factorizing a Gaussian damping factor or using the exact response function does not improve the predictions obtained within this framework. On the other hand, we found that the non-linear 2PI effective action

method overestimates the non-linear power-spectrum on these scales because of the non-linear feedback involved by the coupled system for the response R . However, using the exact non-linear response within this method now improves the agreement with the exact result and can be competitive with the standard perturbation expansion (but this depends on the exact shape of the linear power-spectrum as in our case it is slightly better at $z = 1$ but worse at $z = 0$).

Since the equations of motion associated with the gravitational and the Zeldovich dynamics are very close we can expect these results to apply to the gravitational case. In particular, one can check that is the case at one-loop order, see Valageas (2007). We have found that none of these schemes shows good global convergence properties at high orders. Indeed, they all lead to polynomial or exponential growth into the non-linear regime for the response function, except for the use of Padé approximants which gives bounded response functions with fast oscillations in the highly non-linear regime. On the other hand, non-linear schemes manage to reproduce the damping at one-loop order $p = 1$ but fail at higher orders. Next, no scheme manages to recover the power-law damping of the non-linear matter power-spectrum. They either display increasing growth at higher order or a Gaussian decay which is also somewhat artificial.

On the other hand, an expansion may still be very useful at weakly non-linear scales even if it converges badly (or even diverges) at highly non-linear scales. There, we found that the best methods seem to be the standard perturbation theory or a non-linear expansion where one uses the exact non-linear response (with the Gaussian decay). Thus, these results are somewhat disappointing since it appears to be difficult to build systematic expansion schemes which significantly improve over the standard expansion. One may still obtain some improvement as in Crocce & Scoccimarro (2007) or Matarrese & Pietroni (2007) but this requires some additional ingredients such as the use of an ansatz for the response function which shows a Gaussian decay (but its tentative derivation is not well justified nor systematic) and in some cases for other two-point functions. On the other hand, the use of several expansion schemes can be of interest by itself since they should be accurate at least over the range where they all agree. This allows one to obtain an estimate of their range of validity without the need to perform numerical simulations.

In order to make some further progress, it appears that for observational purposes it may be advantageous to be guided by the expected behavior of two-point functions and to combine such systematic expansions with reasonable ansätze (e.g. Crocce & Scoccimarro 2007). From a theoretical perspective, one may look for different approaches. For instance, one could try to work directly with the Vlasov equation (Valageas 2004). However, this would make the computations significantly more difficult and it is not clear whether it is not more efficient to stick to the hydrodynamical approach and to simply compute higher

order terms, especially if one is mostly interested in weakly non-linear scales. On the other hand, one may consider simpler effective dynamics which attempt to go beyond shell-crossing (based for instance on a Schroedinger equation, Widrow & Kaiser 1993).

References

- Bender C.M., Orszag S.A., 1978, *Advanced mathematical methods for scientists and engineers*, McGraw-Hill Book Co.
- Bernardeau F., Colombi S., Gaztanaga E., Scoccimarro R., 2002, *Phys. Rept.*, 367, 1
- Crocce M., Scoccimarro R., 2006a, *Phys. Rev. D*, 73, 063519
- Crocce M., Scoccimarro R., 2006b, *Phys. Rev. D*, 73, 063520
- Crocce M., Scoccimarro R., 2007, arXiv:0704.2783
- Cvitanovic P., Lautrup B., Pearson R.B., 1978, *Phys. Rev. D*, 18, 1939
- Eisenstein D.J., Hu W., 1998, *ApJ*, 496, 605
- Eisenstein D.J., Hu W., Tegmark M., 1998, *ApJ*, 504, L57
- Eisenstein D.J., et al., 2005, *ApJ*, 633, 560
- Goroff M.H., Grinstein B., Rey S.-J., Wise M.B., 1986, *ApJ*, 311, 6
- Gurbatov S.N., Saichev A.I., Shandarin S.F., 1989, *MNRAS*, 236, 385
- Jain B., Bertschinger E., 1994, *ApJ*, 431, 495
- Jain B., Bertschinger E., 1996, *ApJ*, 456, 43
- Lewis A., Challinor A., Lasenby A., 2000, *ApJ*, 538, 473
- McDonald P., 2007, *Phys. Rev. D*, 75, 043514
- Martin P.C., Siggia E.D., Rose H.A., 1973, *Phys. Rev. A*, 8, 423
- Massey R., et al., 2007, accepted by *ApJ*, astro-ph/0701480
- Munshi D., Valageas P., Van Waerbeke L., Heavens A., 2007, submitted to *Phys. Rep.*, astro-ph/0612667
- Oukbir J., Blanchard A., 1992, 262, L21
- Peebles P.J.E., 1980, *The large scale structure of the universe*, Princeton University Press
- Peebles P.J.E., 1982, *ApJ*, 263, L1
- Phythian R., 1977, *J. Phys. A*, 10, 777
- Schneider P., Bartelmann M., 1995, *MNRAS*, 273, 475
- Scoccimarro R., 2000, *Ann. N.Y. Acad. Sci.*, 927, 13, astro-ph/0008277
- Scoccimarro R., Frieman J., 1996a, *ApJS*, 105, 37
- Scoccimarro R., Frieman J., 1996b, *ApJ*, 473, 620
- Seljak U., 2000, *MNRAS*, 318, 203
- Seljak U., Zaldarriaga M., 1996, *ApJ*, 469, 437
- Shandarin S.F., Zeldovich Y. B., 1989, *Rev. Mod. Phys.*, 61, 185
- Smith R.E., Peacock J.A., Jenkins A., et al., 2003, *MNRAS*, 341, 1311
- Taylor A.N., Hamilton A.J.S., 1996, *MNRAS*, 282, 767
- Valageas P., 2001, *A&A*, 379, 8
- Valageas P., 2002, *A&A*, 382, 477
- Valageas P., 2004, *A&A*, 421, 23
- Valageas P., 2007, *A&A*, 465, 725
- Vishniac E.T., 1983, *MNRAS*, 203, 345
- Widrow L.M., Kaiser N., 1993, *ApJ*, 416, L71
- Younger J.D., Bahcall N.A., Bode P., 2005, *ApJ*, 622, 1
- Zeldovich Y.B., 1970, *A&A*, 5, 84